

THESIS

WALLEYE DERMAL SARCOMA VIRUS ORF C: A POTENTIAL ONCOLYTIC
THERAPY

Submitted by

Elizabeth Magden

Department of Microbiology, Immunology, and Pathology

In partial fulfillment of the requirements

For the Degree of Master of Science

Colorado State University

Fort Collins, Colorado

Summer 2011

Master's Committee:

Advisor: Sandra Quackenbush

Sue VandeWoude
Barbara Biller

Copyright by Elizabeth R. Magden 2011

All Rights Reserved

ABSTRACT

WALLEYE DERMAL SARCOMA VIRUS ORF C: A POTENTIAL ONCOLYTIC THERAPY

Walleye dermal sarcoma virus (WDSV) is a complex retrovirus that causes the growth of multifocal, cutaneous tumors in walleye fish (*Sander vitreus vitreus*). These virus-induced tumors spontaneously regress on a seasonal basis. The WDSV genome encodes three accessory proteins (rv-cyclin, Orf B, and Orf C) that are necessary for regulation of virus expression, tumor formation, and tumor regression. While rv-cyclin and B are critical for tumor development, Orf C contributes to the observed seasonal tumor regression. Previous studies have shown that Orf C targets the cell mitochondria and induces apoptosis. These studies suggest that Orf C-induced apoptosis leads to the observed tumor regression in fish infected with WDSV. To further define the mechanism(s) of apoptosis, we generated a recombinant lentivirus (Lenti Orf C) that expresses WDSV Orf C. By infecting cells with Lenti Orf C, we showed decreasing cell viability in association with increasing virus concentrations. We also demonstrated Orf C expression in mitochondrial, cytosolic, and nuclear cell fractions, with the strongest Orf C expression in cell nuclei. In addition, we identified two pro-apoptotic proteins

that associate with Orf C, ANT and Bax, and identified a third protein, AIF, as a potential Orf C target. While significant progress has been made in elucidating the mechanism(s) of Orf C-induced apoptosis, further studies are necessary to determine which cellular proteins are the primary targets of Orf C. These apoptosis-inducing Orf C targets may be useful in developing future oncolytic therapies.

TABLE OF CONTENTS

Introduction.....	1
Specific AIMS.....	10
Materials and Methods.....	11
Results.....	30
Discussion.....	53
Conclusion.....	65
References.....	67

Introduction

Study significance

Cancer is responsible for 13% of human deaths worldwide (American Cancer Society, 2007). It affects people of all ages, with an increasing risk of most cancer types as people age. Based on cancer incidence rates from 2005-2007, 40.7% of men and women will develop cancer at some point during their lifetime (Altekruse et al., 2010). Given the high incidence of this deadly disease, President Nixon proclaimed a “War on Cancer” in the U.S. in 1971. Since that time the U.S. has invested over \$200 billion into cancer research (Begley, 2008). This investment has resulted in a 5% decrease in cancer-associated mortalities from 1950-2005 (Kolata, 2009). Given the modest nature of cancer decline over the past 50 years, the search for effective cancer therapies continues to be of the utmost importance.

In the quest for an agent to induce cancer cell death, many studies have focused on viruses that cause cell death via apoptosis. Apoptosis is defined as programmed cell death, which is an innate cellular response to infection that limits proliferation of viruses and intracellular bacteria by killing the infected cells. However, some clever infectious agents have evolved ways to express proteins that induce apoptosis, which for them is used as a mechanism of pathogen dispersal and proliferation (Boya et al., 2001). We can potentially use apoptosis-inducing viral pathogens to kill cancer cells by controlling which cells these pathogens target for death.

Under conditions in which cancer cells undergo apoptosis, the term oncolysis is used to describe the destruction of cancer cells. Several viruses have the ability to kill

cancer cells, and researchers have examined these viruses as potential oncolytic treatments. For example, reoviruses are a useful therapy in treating human lymphoid malignancies. Reoviruses target and kill neoplastic cells with an activated Ras-signaling pathway (via mutation of the *ras* oncogene), but leave non-neoplastic cells unharmed (Alain et al., 2002). A second example of an oncolytic virus is an attenuated herpes-simplex-virus mutant that induces tumor cell regression in human neural tumors (Kesari et al., 1995). Another virus that may offer similar oncolytic potential is a walleye virus, called walleye dermal sarcoma virus (WDSV). Initial studies show WDSV causes cell apoptosis (Nudson et al., 2003). Further characterization of this walleye virus is necessary to determine its potential as an effective oncolytic therapy.

WDSV Background

Walleye dermal sarcoma virus is a type-C retrovirus (Martineau et al., 1991; Martineau et al., 1992) that infects walleye fish (*Sander vitreus vitreus*) throughout North America. The virus induces skin lesions that range from epidermal hyperplasia to dermal sarcoma (Walker, 1969). Walleye dermal sarcomas (WDS) are grossly identifiable as clusters of spherical nodules (2-5 mm) with either a smooth or ulcerated surface. The tumors are found multifocally on any region of the skin, and are generally non-invasive. Microscopically the tumors show a defined demarcation from the dermis and a variable cellularity. The sarcomas show whorls of fibroblast-like cells with abundant basophilic cytoplasm (Martineau et al., 1990b). Some of the tumors exhibit the presence of

intracellular osteoid material. Often lymphocytic inflammation is present to varying degrees in the dermis adjacent to the tumor (Martineau et al., 1990b).

Since the initial discovery of walleye dermal sarcoma, much has been discovered about its cause and pathogenesis. The lymphocytic inflammatory response observed in dermal sarcomas is most pronounced in fish collected during the spring and summer, with minimal inflammation present in those fish collected during the fall (Bowser et al., 1988). The inflammatory response does not correlate with the seasonal prevalence of the tumors themselves, as the dermal sarcomas are more prevalent in the fall and spring versus summer (Bowser et al., 1988). This difference in seasonal prevalence of tumor growth may be correlated with water temperature, although other host and environmental factors likely contribute to disease. Experimental transmission studies demonstrated that 15°C was the optimal temperature for tumor growth, suggesting that as the water temperature drops in the fall conditions are ideal for tumor development (Bowser et al., 1990).

To further examine the difference in seasonal prevalence, experimental virus transmission was attempted using cell-free inocula from tumors harvested in the spring versus fall. Only the inocula derived from spring tumors produced transmissible tumors (Bowser et al., 1996). Additional analyses found that only the spring tumors harbored high levels of virus, while the fall tumors contained little to no virus (Martineau et al., 1992; Bowser et al., 1996).

The experimental transmission of WDS to walleye further supports the theory that the dermal sarcoma lesion is caused by a virus. A study by Holzschu et al. (1997b), demonstrated 100% tumor growth in 14 week old walleye fish that were inoculated

intramuscularly with WDS cell free filtrates. These transmissibility experiments also demonstrated that the tumors formed via virus inoculation were generally non-invasive and restricted to the dermis (Marineau et al., 1990a; Holzschu et al., 1997b).

While nearly all feral observations of these dermal sarcomas have demonstrated a benign presentation, experimental infection of young walleye fingerlings show a higher prevalence of invasive neoplasms. One study using 9 week old fingerlings demonstrated an occasional locally invasive neoplasm following intramuscular inoculation (Earnest-Koons et al., 1996). A second study using slightly younger fingerlings (6-8 weeks) found 100% of 6-8 week old fingerlings developed invasive tumors when inoculated intramuscularly (Bowser et al., 1997). The formation of this invasive tumor may be related to the young age of the walleye at time of initial infection, stressful housing conditions, and/or captive diet (Earnest-Koons et al., 1996). A more recent study also found invasive WDS tumor in three adult walleye fish (Bowser et al., 2002), but this finding remains rare.

One of the most interesting WDS characteristics is that the tumors regress in the spring/summer, and this regression can be in part be correlated to an increasing water temperature (Bowser and Wooster, 1991; Getchell et al., 2000a). Once the tumor regresses, the walleye fish develop resistance to the virus and have a much lower probability of tumor redevelopment (Getchell et al., 2000b; Getchell et al., 2001). This tumor regression occurs via apoptosis (Quackenbush et al., 2001; Nudson et al., 2003; Rovnak and Quackenbush, 2010). Further study of the specific genes causing the tumor regression is particularly important to characterize the therapeutic properties of this virus.

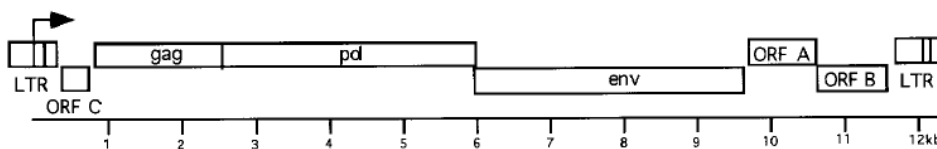
WDSV molecular structure

It was confirmed in 1991 that a type-C retrovirus was present in walleye dermal sarcomas using molecular techniques and likely the etiological agent (Martineau et al., 1991; Martineau et al., 1992). This proposed etiology was further supported by the detection of abundant viral transcripts within the neoplastic tumor cells (Poulet et al., 1995). Retroviruses can play a role in tumorigenesis via their ability to convert RNA genome to double-stranded DNA that can integrate into the host genome and convert proto-oncogenes into oncogenes via retroviral transduction (Bowser and Casey, 1993).

WDSV is also unique in that it contains high levels of un-integrated viral DNA, a rarity among oncovirus-induced tumors (Bowser and Casey, 1993; Martineau, 1992). High virus levels are found in tissues from regressing spring tumors. The regressing spring tumors yielded 10-50 copies of viral DNA per cell. In contrast, less than one copy of viral DNA per cell was isolated from the developing fall tumors (Bowser et al., 1996). The regressing spring tumors contained the full length genomic RNA, while it was undetectable in the developing fall tumors (Bowser et al., 1996; Martineau et al., 1991; Martineau et al., 1992). In addition, the fall tumors only express two spliced transcripts, while the spring tumors express these two spliced transcripts plus spliced *env* and the full length genomic RNA (Quackenbush et al., 1997). There is also a significant quantitative difference in the expression of these subgenomic transcripts between the two seasons, with the viral mRNA from spring tumors demonstrating levels up to 100x greater than those present in fall tumors (Quackenbush et al., 1997).

The entire nucleotide sequence of a DNA clone of walleye dermal sarcoma virus has been determined and shows several distinguishing features within its 12,708 bp sequence (Holzschu et al., 1995; Holzschu et al., 1997a). Long terminal repeats (LTRs) measuring 590 bp bracket each end. The LTRs contain a U3 region of 440 bp, a 77 bp R region and a 73 bp U5 region, with the start site of transcription located at the junction between the U3 and R regions. Also present in the LTR are a consensus polyadenylation sequence and TATA box. Another unique molecular characteristic of WDSV is that in addition to encoding the open reading frames (ORFs) present in all retroviruses, *gag*, *pol*, and *env*, it also contains three accessory genes *orf A*, *orf B*, and *orf C*. Orf A and Orf B are located between the *env* gene and the 3' LTR, while Orf C is found in the leader region between the *gag* gene and the 5' LTR (Holzschu et al., 1995; Holzschu et al., 1997a).

WDSV genomic structure



(Quackenbush et al., 1997)

WDSV Orf A encodes the protein rv-cyclin that is specifically expressed at the time of tumor development (Rovnak et al., 2001). This finding suggests that rv-cyclin plays a role in WDS induction. It has additionally been shown that rv-cyclin localizes to the cell nucleus and is concentrated in the interchromatin granules, potentially affecting

mRNA transcription (Rovnak et al., 2001). Transcription has been shown to be affected via the direct interaction between rv-cyclin and TAF9 (Rovnak and Quackenbush, 2006), which interferes with NF- κ B and downregulates NF- κ B-dependent transcription (Quackenbush et al., 2009), potentially contributing to tumorigenesis.

Additional evidence suggesting a role of rv-cyclin in tumor development is that rv-cyclin affects cell growth (LaPierre et al., 1998; Lairmore et al., 2000, Brewster et al., 2011). WDSV rv-cyclin enhances host gene expression and proliferation of mammalian cells and is able to rescue cyclin-deficient yeast from growth arrest (LaPierre et al., 1998; Brewster et al., 2011). Further support exists in the finding that rv-cyclin induces a squamous epithelial hyperplasia in transgenic mice (Lairmore et al., 2000).

Orf B localizes to the cell cytoplasm (Rovnak et al., 2007). In this location Orf B directly interacts with the receptor for activated C kinase (RACK1) and activates protein kinase C (PKC) (Daniels et al., 2008). PKC serves a wide variety of functions, ranging from cell proliferation to apoptosis (Nakashima, 2002). In Orf B expressing cells, the activation of PKC appears to convey a cellular ability to survive, and even proliferate, in serum-deprived conditions (Daniels et al., 2008). Both rv-cyclin and Orf B are expressed in the developing fall tumors, indicating these genes may play a role in tumor development (Quackenbush et al., 2001).

Orf C is encoded by the full-length genomic RNA, which is expressed at very high levels during tumor regression (Quackenbush et al., 1997; Quackenbush et al., 2001). Orf C localizes to the cell mitochondria and causes an alteration in mitochondrial membrane potential (Nudson et al., 2003), which may then trigger apoptosis. Cells

expressing Orf C exhibit a distinctly different morphology and loss of membrane integrity, further evidence that Orf C is associated with induction of apoptosis. Additionally, cells transfected with an Orf C expression construct and stained with Annexin V (an apoptosis-indicator) show increasing levels of apoptosis over 48 hours when compared to rv-cyclin expressing cells (Nudson et al., 2003). The apoptotic ability of Orf C supports the theory that Orf C expression from the full length genome plays a significant role in tumor regression via an apoptotic pathway.

Orf C - mechanisms of apoptosis

Mitochondria have been shown to play a critical role in the process of apoptosis via the extrinsic or intrinsic pathways. When the extrinsic pathway is initiated, apoptosis occurs via death receptors expressed at the cell surface that activate caspases which alter the mitochondrial membrane potential (MMP), while the intrinsic pathway initiates intracellular death signals that target the mitochondria directly and alter the MMP prior to caspase activation (Boya et al., 2004; Brenner et al., 2000; Everett et al., 2001; Green et al., 1998; Kroemer et al., 1998; Reed et al., 2000).

Both extrinsic and intrinsic apoptosis pathways generally either involve proteins from the caspase family and/or the Bcl-2 family. During mitochondrial targeted apoptosis proteins from the inter-membrane space between the inner and outer mitochondrial membranes, such as cytochrome c, leak into the cell cytosol. These leaked proteins will activate procaspase-9, which in turn activates the pro-apoptotic protein, caspase 3. The cell mitochondria will also release other apoptosis activators such as

apoptosis-inducing factor, AIF (Everett et al., 2001; Martinou et al., 2001; Zamzami et al., 2001). The pro-apoptotic proteins in the Bcl-2 family include Bax, Bak, and Bid. Activation of these Bcl-2 proteins acts as a junction between the extrinsic and intrinsic pathways that amplifies the apoptosis process (Everett et al., 2001; Heibein et al., 2000).

In addition to the pro-apoptotic Bcl-2 proteins and caspases, other pro-apoptotic stimulators include non-proteinaceous factors such as fatty acids or nitric oxide and transcription factors such as p53 and NGF1 β (Boya et al., 2001). These apoptosis initiating signals can target a wide variety of mitochondrial membrane receptors including lipid rafts, cardiolipin, adenine nucleotide translocase (ANT), and voltage-dependent anion channel (VDAC) (Boya et al., 2001). As these membrane receptors are targeted, there is a corresponding loss of electrochemical potential across the inner mitochondrial membrane due to the opening of the permeability transition (PT) pore (Zamzami et al., 2001). The PT pore is comprised of the voltage-dependent anion carrier (VDAC) in the outer mitochondrial membrane, adenine nucleotide translocase (ANT) in the inner mitochondrial membrane, and cyclophilin D (CPD) which is closely associated with ANT (Crompton, 1999). Thus far, all the virus-associated pro-apoptotic proteins have amphipathic α -helices with pore-forming properties (Boya et al., 2004). It is likely that WDSV Orf C induces apoptosis via one of these pro-apoptotic pathways, ultimately leading to the observed seasonal tumor regression.

Given the ability of WDSV Orf C to induce apoptosis, the goal of this study is to determine the mechanism(s) of Orf C-induced apoptosis and use this oncolytic property to target and kill tumor cells. By studying cellular infection and potential mechanism(s)

by which WDSV Orf C induces apoptosis, we can gain information necessary to develop an effective oncolytic therapy.

Specific AIMS

WDSV is known to express the viral accessory protein, Orf C, at the time of tumor regression. Previous work has demonstrated that Orf C targets cell mitochondria and affects the mitochondrial membrane potential (Nudson et al., 2003). It has also been shown that Orf C expressing cells undergo apoptosis (Nudson et al., 2003). Based on these previous observations we hypothesize that Orf C interacts with the permeability transition pore complex (PTPC) to initiate apoptosis. We have outlined several AIMS and associated goals to test this hypothesis.

AIM 1. To construct a recombinant lentivirus expressing WDSV Orf C and assess its affect on cell growth.

We used the pLVX-Puro Vector (Clontech®), a lentiviral expression vector based on human immunodeficiency virus-1, to express WDSV Orf C. To evaluate the apoptosis potential of our recombinant Orf C-expressing lentivirus we used an in vitro assay to screen various cell lines for use in our in vitro experiments.

AIM 2. To determine the subcellular localization of the lentivirus expressed Orf C

We assessed Orf C expression in mitochondrial, nuclear, and cytosolic cell fractions following infection with Lenti Orf C virus.

AIM 3. To determine the mechanism of Orf C-induced apoptosis.

Caspase activation in Orf C-expressing cells

We examined several caspases (3, 6, 9, and 12) to determine if Orf C induces apoptosis via a caspase-dependent or caspase-independent pathway, and to show which pathway may be activated. Specifically, we looked for the activated cleaved caspases in association with Orf C expression.

Identification of Orf C interacting proteins

We analyzed transition pore complex proteins VDAC (voltage-dependent anion channel) and ANT (adenine nucleotide translocase) for potential interaction with Orf C. We also conducted in vitro experiments evaluating the potential activation of several pro-apoptotic proteins (Bcl-2, Bax, AIF).

AIM 4. To assess Orf C's potential as an oncolytic therapy.

Once the mechanism of Orf C-induced apoptosis has been determined, we propose an experiment analyzing the potential in vivo use of Orf C as an oncolytic therapy.

Materials and Methods

Recombinant lentivirus expression system

The pLVX-Puro Vector (Clontech®) is a lentiviral expression vector based on human immunodeficiency virus-1. We used this lentiviral vector to express our gene of

interest, WDSV Orf C, as this expression system is more efficient than standard transfections. We also used the empty lentiviral vector as an experimental control. Gene expression with this system is driven by a cytomegalovirus (CMV) promoter located upstream from the multiple cloning site (MCS). The pLVX-Puro Vector is 8102 base pairs and contains both a puromycin resistance gene, for selection of stable transductants in mammalian cells, and an ampicillin resistance gene for propagation and selection in bacteria.

The insert, Orf C, was excised from the pKH3-Orf C expression construct (Nudson et al., 2003). Two μg were digested with SalI and ClaI (NEBuffer 2 (New England BioLabs, Inc.; 50 mM NaCl, 10 mM Tris-HCl, 10 mM MgCl₂, 1 mM Dithiothreitol, pH 7.9), 1x BSA (bovine serum albumin)) and incubated at 37 °C overnight. The pLVX-Puro vector (two μg) was digested with compatible enzymes XhoI and BstBI (NEBuffer 4 (New England BioLabs, Inc., 50 mM potassium acetate, 20 mM Tris-acetate, 10 mM magnesium acetate, 1 mM Dithiothreitol, pH 7.9), 1x BSA) and incubated at 37°C overnight.

Digests were separated on a 1% agarose TAE (0.04 M Tris-acetate, and 1 mM ethylenediaminetetraacetic acid (EDTA) and glacial acetic acid) gel run at 70 volts for 90 minutes. The appropriate bands were cut out: 357 bp for Orf C and 8.1 kb for pLVX-Puro vector. DNA was extracted from the gel with the Qiagen® QIAquick Gel Extraction Kit. Gel slices were combined with three times the volume of QG buffer (Qiagen® solubilization and binding buffer) and incubated at 50°C for ten minutes to dissolve agarose. Mixture was applied to the QIAquick® spin column. The nucleic acids adsorbed to the silica-gel membrane and the column was spun for one minute. Impurities

were rinsed away with 750 μ L of PE wash (Qiagen® wash buffer, 10 mM Tris-HCl pH 7.5, 80% ethanol) and column was spun again for one minute. Excess alcohol was removed with a final 90 second spin. DNA was eluted with 50 μ L of EB buffer (Qiagen® elution buffer; 10 mM Tris-Cl, pH 8.5) and the column was spun for one minute. Purified DNA was quantitated on an ethidium bromide agarose gel by comparing to the NEB 1 kb ladder as a standard.

Ligation was performed with 50 ng of digested pLVX puro vector plus 7.5 ng Orf C insert (3:1 molar ratio) with NEB T4 ligase (New England BioLabs, Inc.) in 1x ligase buffer (50 mM Tris-HCl, 10 mM $MgCl_2$, 1 mM ATP, 10 mM Dithiothreitol, pH 7.5) in 15 μ L and incubated overnight at 4°C. JM109 *E.coli* chemically competent cells were used for the transformation. Five μ L of the ligation was added to 100 μ L of JM109 cells and placed on ice for 30 minutes. The cells and ligation were next heated to 42°C for 45 seconds, and then placed on ice for two minutes. Super optimal broth (SOB) (0.5 mL) (Bacto-tryptone 2%, yeast extract 0.5%, NaCl 0.005%, KCl 2.5 mM, 10mM $MgCl_2$ pH 7.0) was added to the tube and shaken at 37°C for 90 minutes. Next the mixture was spread on LB (Lysogeny Broth) ampicillin plates (Tryptone 1%, yeast extract 0.5%, NaCl 1%, Agar 1.5%, 0.1 mg/mL ampicillin) and incubated overnight at 37°C. One colony was observed the following day. The single colony was harvested and placed in 100 mL LB-amp overnight at 37°C with shaking (250 rpm).

Following overnight LB-amp growth the plasmid was isolated with Promega's Pure Yield™ Midiprep System kit. The cultures were centrifuged (Sorvall® RC6 with S534 rotor at 9,000 x g for ten minutes) and the resulting pellet was resuspended in three mL resuspension buffer (50 mM Tris-HCl (pH 7.5), 10 mM EDTA (pH 8.0), 100 μ g/mL

RNase A) by vortexing. Next, three mL cell lysis buffer (0.2 M NaOH, 1% SDS) was added and maintained at room temperature for three minutes, followed by the addition of five mL neutralization buffer (4.09 M guanidine hydrochloride (pH 4.8), 759 mM potassium acetate, 2.12 M glacial acetic acid) to precipitate genomic DNA and protein structure. The tubes were then incubated at room temperature for three minutes.

The precipitated bacterial lysate was clarified by pouring into a clearing column and allowed to incubate three minutes before vacuum pressure was applied to the column. The DNA containing flow-through passed onto a DNA binding column and the vacuum was slowly released. Next, the membrane-bound DNA was washed by adding five mL endotoxin removal wash (Promega PureYield™ Plasmid Midiprep System) and vacuum pressure was reapplied. Column wash (20 mL) (162.8 mM potassium acetate, 22.6 mM Tris-HCl (pH 7.5), 0.109 mM EDTA (pH 8.0) with 95% ethanol added before use to a final concentration of 60% ethanol, 60 mM potassium acetate, 8.3 mM Tris-HCl, and 0.04 EDTA) was added and vacuum pressure was again applied. The membrane was dried by applying vacuum for 30 seconds. The DNA was eluted from the membrane with 600 μ L of nuclease-free water. The Eppendorf BioPhotometer 6131 was used to determine the concentration of purified DNA (546.4 μ g/mL) by absorbance at 260 nm.

Next, restriction digests were performed to confirm the presence of Orf C. Since compatible enzymes were used for initial cloning (SallI-XhoI and BstBI-ClaI) they could not be used to recut for confirmation of appropriate insert. We instead used EcoRI and KpnI digests to screen the clone for insertion and correct orientation and separated the digest on a 2% agarose TAE gel at 100 volts. The resulting banding patterns matched those expected for pLVX-puro with an Orf C insert. The correct ligation would liberate a

200 bp fragment with EcoRI and correct orientation was confirmed with a 100 bp fragment with KpnI. Sequence was further confirmed via DNA sequencing.

Lenti Orf C virus production.

The Lenti-X™ HT Packaging System, along with Lenti-X™ 293T cell line, was originally used for the production of both Lenti Orf C and Lenti empty vector viruses, following the protocol from Clontech Laboratories, Inc. entitled, “Protocol: Lentiphos™ HT Protocol.” We followed the same procedure at a later date using the Lenti-X™ HT Ecotropic Packaging system to produce ecotropic Lenti Orf C and ecotropic Lenti empty vector viruses (ecotropic envelope glycoprotein (gp70)). Both protocols involved adding 4×10^6 Lenti-X™ 293 T cells in 10 mL of Dulbecco’s modified Eagle medium (DMEM/High Glucose, Hyclone® ThermoFisher; 4 mM L-glutamine, 4500 mg/L glucose, -sodium pyruvate) with 10% fetal bovine serum (FBS) (Benchmark™, Gemini Bio-Products) to 100 mm tissue culture plates 24 hours prior to transfection. Plates were incubated at 37°C overnight (24 hours) in 5% CO₂. Lenti Orf C plasmid DNA (three µg) was added to 15 µL of Lenti-X™ HT Packaging Mix or Lenti-X™ HT Ecotropic Packaging system and 423 µL sterile H₂O into 12 x 75 mm polystyrene tubes. Lentiphos1 solution (62 µL) was added to the diluted Lenti Orf C plasmid DNA and vortexed thoroughly. While vortexing the DNA/Lentiphos1 solution, Lentiphos2 (500 µL) was added dropwise into the tube. The mixture was incubated at room temperature for ten minutes to allow DNA precipitate to form. The solution was then gently vortexed and entire contents were added to the 293T cells in DMEM with 10% FBS and plates

were incubated overnight at 37°C. Following the 24 hour incubation period, the transfection medium was aspirated and replaced with 10 mL of fresh cell culture medium and plates were incubated an additional 48 hours at 37°C. Following this 48 hour incubation, supernatants were collected, centrifuged at 500 x g for ten minutes to remove cellular debris, aliquoted, and stored at -80°C.

Following virus production, virus titrations were performed using HeLa cells infected with 10-fold dilutions of Lenti Orf C or Lenti empty vector virus in DMEM with 10% FBS. Polybrene (8 µg/mL) (hexadimethrine bromide) was added to the cell culture media to enhance infectivity. Twenty-four hours post transfection, virus and media were aspirated and puromycin (5 µg/mL) selection began. Antibiotic resistant colonies were allowed to grow for 10-14 days with fresh media changes occurring every two or three days. All media was then aspirated and cell colonies were stained with 1% crystal violet solution in EtOH and enumerated.

Due to low virus titers, FuGene® 6 Transfection Reagent (Roche) was also used to grow virus in an attempt to achieve higher viral titers. For these transfections, we combined 835 µL of Opti-MEM® (Invitrogen™) with 25 µL FuGene® (Roche) and incubated at room temperature for five minutes. We then added a DNA mixture containing Lenti Orf C (3.4 µg), and the packaging plasmids pLP/VSV-G (1.2 µg) (Vesicular Stomatitis Virus G glycoprotein; 1 µg/mL in TE buffer (Tris 10 mM, EDTA 1 mM)), pLp1 (encodes *gag/pol*; 1 µg/mL in TE buffer) (3.7 µg), and pLp2 (encodes *rev*; 1 µg/mL in TE buffer) (1.7 µg) to the Opti-MEM®/FuGene® solution and incubated another 15 minutes. The entire mixture was added to the 293T cells/media and incubated at 37°C for 48 hours. Following the 48 hour incubation period the resulting supernatant

was harvested, centrifuged at 500 x g for 15 minutes to remove cellular debris, and stored at -80°C. Due to a failed lot of FuGene® 6 Transfection Reagent (Roche), we substituted an improved FuGene® HD Transfection Reagent (Roche) for virus production later in the study.

Ultracentrifugation was used to further increase our virus concentrations. Viral supernatants were added to Ultra-Clear™ Beckman centrifuge tubes (25 x 89 mm) and balanced centrifuge tubes were placed in a cooled SW-28 swinging bucket rotor. Tubes were centrifuged at 16,500 rpm (30,500 x g) for 90 minutes and the resulting viral pellet was resuspended in 1/100th of original volume of filtered cold TNE solution (10 mM Tris, 0.1 M NaCl, 1 mM Na₂EDTA, adjust to pH of 7.5 with HCl) and virus was stored at -80°C.

In vitro assessment of the effect of Orf C on cell growth

To assess the effect of Orf C expression on cell growth, we performed cell viability assays using a variety of cell types. We analyzed the effect of Orf C on the growth of 4T1, MCA-205, and NIH-3T3 cells in order to establish which cell line would function best as a model of Orf C-induced apoptosis. In 96-well tissue culture plates, 2500 cells were plated per well, with 42 wells of each cell type and 12 wells left blank to measure background absorbance. Experimental samples consisted of 6 wells each of uninfected cells, Lenti empty vector infected cells at multiplicity of infection (MOI) of 5, 10, and 20, and cells infected with Lenti Orf C at the same virus concentrations (results note when different MOIs and sample sizes were used). The experiment was setup in

triplicate in order to assess cell viability at three different time points: 24, 48, and 72 hours post-infection. The virus was added to the wells along with media (DMEM with 10% FBS) plus polybrene (8 µg/mL) in a total volume of 100 µL per well. The tissue culture plates were incubated overnight at 37°C.

Twenty-four hours post-infection the first set of 96 well plates were analyzed for cell viability using CellTiter96® Aqueous One Solution Cell Proliferation Assay (MTS) (Promega™). The media from each individual well was aspirated and replaced with 100 µL of fresh DMEM with 10% FBS. We then added 20 µL of the CellTiter96® Aqueous One Solution Reagent to the cultured cells. The plates were incubated for 1-3 hours at 37°C in a humidified chamber in 5% CO₂. The resulting absorbance was then recorded at 490 nm using the Beckman Coulter™ LD 400 plate reader.

The virus and media from the remaining tissue culture plates (48- and 72-hour incubation periods) were aspirated and 200 µL of fresh media (DMEM with 10% FBS) was added to each well. The same cell viability assay procedure was used for these tissue culture plates at 48 and 72 hours post-infection.

This cell viability experiment was repeated one time using the CellTiter-Blue® Cell Viability Assay (Promega™). Cells (2×10^3 4T1 and NIH-3T3 cells) were plated in a 96-well opaque black plate suitable for cell culture with 200 µL of DMEM with 10% FBS. Cells were infected with Lenti Orf C or Lenti empty vector virus (VSVG) at a MOI of 0, 1, 5, or 10 (n=3, due to virus volume constraints) and incubated for 48 hours at 37°C. CellTiter-Blue® Reagent (20 µL/well) was added and plate was shaken for ten seconds and then incubated at 37°C for two hours. The 96-well plate was shaken again

for ten seconds and resulting absorbance was recorded at 560/590 nm using a fluorescent plate reader.

Statistical analyses were performed using a one-sided two-sample student's t-test, with significance set at p-value < 0.05.

Subcellular localization of the lentivirus expressed Orf C

To demonstrate subcellular localization of Orf C, HeLa cells were transfected with pKH3 or pKH3-Orf C. For these transfections, we combined 500 μ L of Opti-MEM® (Invitrogen™) with 40 μ L FuGene® HD (Roche) and incubated at room temperature for five minutes. We then added 10 μ g of DNA (pKH3 or pKH3-OrfC) to the Opti-MEM®/FuGene® mixture and incubated at room temperature for 15 minutes. The complete mixture was gradually dripped onto a 100 mm tissue culture plate of HeLa cells (3×10^6 cells) that had been plated the previous day, and the transfected cells were incubated at 37°C with 10 mL of DMEM with 10% FBS for a total of 48 hours.

At 48 hours post-transfection all media was aspirated, cells were rinsed with Phosphate buffered saline (PBS; 137 mM NaCl, 2.7 mM KCl, 4.3 mM Na₂HPO₄, 1.47 mM KH₂PO₄, adjust to pH 7.4), and trypsin (0.05% plus EDTA in Hanks Balanced Salt Solution (HBSS); 0.137 M NaCl, 5.4 mM KCl, 0.25 mM Na₂HPO₄, 0.44 mM KH₂PO₄, 1.3 mM CaCl₂, 1.0 mM MgSO₄, 4.2 mM NaHCO₃) was added to the cells. Cells were harvested and transferred to a 50 mL conical tube, and centrifuged at 500 x g for five minutes. Cells were then washed twice with 10 mL of PBS and re-centrifuged at 500 x g for five minutes.

Mitochondrial, nuclear, and cytosolic cells fractions were then isolated following the MitoProfile® benchtop mitochondrial isolation kit for cultured cells (Mitosciences®). Following cell collection and wash, the cells were placed at -80°C to freeze cells, and then thawed on ice to weaken the cell membranes. The cells were then resuspended in five mg/mL Reagent A with added proteinase inhibitor (Sigma) (ten µL/mL) and PMSF (phenylmethanesulfonylfluoride) (two µL/mL), and incubated on ice for ten minutes. The cells were transferred to a pre-cooled Dounce homogenizer and homogenized using 20 strokes with a B pestle. The homogenate was transferred to a centrifuge tube and centrifuged at 1,000 x g for ten minutes at 4°C. The resulting supernatant was saved as supernatant #1.

The resulting pellet was resuspended in Reagent B with added proteinase inhibitor and PMSF with the same volume used as Reagent A. The same rupturing and spin steps were repeated as with Reagent A. The pellet resulting from this second spin cycle constituted the nuclear cell fraction. Nuclear cell fractions were gently washed twice with Reagent B by resuspending the nuclear pellet in 1 mL of buffer, centrifuging at 1500 x g for three minutes, and then adding Dignam C extraction buffer (20 mM HEPES (pH 7.9), 25% (v/v) glycerol, 0.42 M NaCl, 1.5 M MgCl₂, 0.2 mM EDTA, 0.5 mM PMSF, 0.5 mM DTT) at two volumes buffer: one volume nuclear pellet. The pellet was rotated overnight at 4°C and samples were then frozen at -80°C.

The supernatant (supernatant #2) was combined with supernatant #1, mixed thoroughly, and centrifuged at 12,000 x g for 15 minutes at 4°C. The resulting supernatant from this final centrifuge was saved as the cytosolic cell fraction. The resulting mitochondrial pellet was resuspended in an equivalent volume (one volume of

cell pellet) of Chaps® Cell Extract Buffer (Cell Signaling Technology®) (0.1% Chaps, 50 mM Pipes/HCl (pH 6.5), 2 mM EDTA, 20 µg/mL Leupeptin, 10 µg/mL Pepstatin A 10 µg/mL Aprotinin, 5mM DTT). Resuspended mitochondria were frozen at -80°C and thawed twice on ice, followed by centrifugation at 14,000 rpm at 4°C for five minutes to lyse mitochondria. Samples were frozen at -80°C.

To determine the subcellular localization of Orf C following infection, four different cell types were infected with either Lenti Orf C, Lenti empty vector, or remained un-infected as a control. The cell types used were: 4T1 cells, a mouse mammary tumor cell line; HeLa cells; NIH-3T3 cells, a mouse fibroblast line; and MCA-205 cells, a mouse sarcoma cell line. The 4T1 and MCA-205 cells were of most interest as a potential cancer cell line in which we could demonstrate apoptosis.

Using 6-well tissue culture plates, 3 wells of each cell line were plated at a concentration of 2×10^5 cells/well. One well was left uninfected, one well was infected with Lenti empty vector virus, and one well was infected with Lenti Orf C virus. The virus concentration used for each experiment varied as indicated in the results section. The total volume of virus, media (DMEM with 10% FBS), and polybrene (8 µg/mL) was 1 mL/well. The tissue culture plates were incubated overnight at 37°C. At 24 hours post-infection, trypsin was added to the cells and each well was split into two 100 mm tissue culture plates. DMEM with 10% FBS was added to each plate (ten mL) and incubated for 48 additional hours. Cells were harvested by trypsinizing cells, transferring cells to a 50 mL conical tube, and centrifuging at 500 x g for five minutes. Cells were rinsed with PBS and re-centrifuged at 500 x g for five minutes (x2). Mitochondrial, nuclear, and cytosolic cells fractions were then isolated following the MitoProfile®

benchtop mitochondrial isolation kit for cultured cells (Mitosciences®), as described above.

Protein concentrations for the various cell fractions were determined using a Micro BCA™ protein assay kit (Thermoscientific®), microplate procedure. Micro BCA Working Reagent (WR) was prepared by mixing 25 parts Micro BCA Reagent MA, 24 parts Micro BCA Reagent MB, and one part Reagent MC. We added 150 µL of WR to a 96 well plate plus 150 µL of the diluted standards or samples (148 µL millQ H₂O plus two µL sample or standard). The plate was incubated at 37°C for two hours, cooled to room temperature, and the absorbance was measured at 562 nm on a Beckman Coulter™ LD 400 plate reader.

Fifteen µg of each sample was run on a 12-well, 12% acrylamide gel with 200 mL MES buffer (2-(N-morpholino) ethanesulfonic acid) plus 0.5 mL NuPAGE® antioxidant at 200 V constant for 50 minutes. Proteins were transferred to an Immobilon™ transfer membrane (Millipore™) and run at 150 mAmps constant for two hours. The membrane was rinsed with Tris-buffered saline (TBS) buffer (25 mM Tris) for five minutes and placed in blotto (a milk diluents/blocking solution – 5% Carnation® instant non-fat dry milk, 10% 10x PBS, 0.0025% Tween 20, in TBS wash) for 30 minutes followed by three consecutive washings in TBS buffer for five minutes each. The primary antibody (XHA 12CA5, 1:1000) was added to the membrane and incubated at 4°C overnight with rocking. The following day the membrane was rinsed with TBS buffer three times for five minutes each and the secondary antibody (G x M IgG HRP, 3:5000) was applied. The membrane was incubated with the secondary antibody for one hour at room

temperature with rocking, rinsed again with TBS buffer (three times, five minutes each), and developed with TMB western blot kit (KPL™).

TMB Peroxidase Substrate (625 µL), Peroxidase Substrate Solution B (625 µL), and TMB Membrane Enhancer (125 µL) were mixed in a 5:5:1 ratio. This solution was placed on the rinsed membrane for one hour with a clear plastic sheet on top to prevent solution evaporation. The developed membrane was then scanned (Visoneer® OneTouch™ 9400) and the image adjusted with Adobe Photoshop® CS (Version 8.0, 2003).

Mechanisms of Orf C-induced apoptosis

Caspase activation in Orf C-expressing cells. Using a 6-well tissue culture plate, 2×10^5 cells from both the 4T1 and NIH-3T3 lines were plated in three wells each. For each cell line one well was uninfected, one well was infected with Lenti empty vector virus and one was infected with Lenti Orf C virus at a MOI of five to ten. Virus was added to media (DMEM with 10% FBS) plus polybrene (8 µg/mL) to a total volume of 1 mL/well. Twenty-four hours post-infection the cells were split into a 100 mm tissue culture plate and incubated an additional 24 hours. Next, the cells were harvested using trypsin and ten mL DMEM with 10% FBS was added. The cell containing solution was centrifuged at 500 x g for five minutes. The resulting cellular pellet was rinsed with 10 mL PBS followed by centrifugation at 500 x g for five minutes (x2).

All PBS was aspirated from the cellular pellet and cells were resuspended in immunoprecipitation (IP) buffer (1% Triton X-100, 150 mM NaCl, 10 MM Tris (pH 7.4,

1 mM EDTA, 1 mM EGTA (ethylene glycol tetraacetic acid), 0.2 mM sodium orthovanadate, 0.2 mM PMSF, 0.5% Nonidet NP-40 (octyl phenolpolyethoxyethanol)) and incubated at 4°C with rotation overnight. In a duplicate experiment the same protocol was used but Chaps® Cell Extract buffer (1 volume buffer:1 volume cell pellet) (Cell Signaling Technology®, #9852) (50 mM Pipes/HCl (pH 6.5) 2 mM EDTA, 0.1% Chaps, 20 µg/mL Leupeptin, 10 µg/mL Pepstatin A, 10 µg/mL Aprotinin, with DTT (Dithiothreitol) added to 5 mM) was used in place of the IP buffer used in the original experiment. Cells were centrifuged at 14,000 rpm for ten minutes and the supernatant was collected. A Micro BCA™ protein assay was performed to determine the protein concentrations. Fifteen µg of protein was loaded from each sample onto a Nu-PAGE® Bis-Tris 12% acrylamide gel (10 well) and run at 200 V constant for 50 minutes. Proteins were transferred to an Immobilon™ transfer membrane (Millipore™) and run at 150 mAmps constant for two hours. The membrane was rinsed with TBS wash for five minutes and incubated in blotto at room temperature for one hour.

Following incubation in blotto and three subsequent washes (5 minutes each) with TBS buffer, a variety of primary antibodies for caspase detection were applied using the Apoptosis Antibody Sampler Kit (Mouse Specific) from Cell Signaling Technologies® (#9930). The primary antibodies used included: caspase-3, cleaved caspase-3 (Asp175) (5A1E) Rabbit mAb, caspase-12, caspase-6, cleaved caspase-6 (Asp162), caspase-9, cleaved caspase-9 (Asp353), and cleaved-PARP (Poly(ADP-ribose)polymerase) (Asp214). The primary antibodies were diluted to 1:1000 in primary antibody dilution buffer (0.5% BSA, 1% 10x TBS, and 90% MilliQ H₂O; add 100% Tween 20). The secondary antibody used for all caspase detection western blots was Anti-Rb IgG, HRP-

linked (diluted 1:2000 in primary antibody dilution buffer). The primary antibody was incubated with the membrane overnight at 4°C with gentle rocking. Following three washes with TBS buffer, the secondary antibody was applied and incubated at room temperature for one hour. The membranes were then developed with TMB western blot kit (KPL™) as previously described.

Identification of Orf C interacting proteins. Adenine nucleotide translocase (ANT), voltage-dependent anion channel (VDAC), Bcl-2 (pro-apoptotic protein), and Bax (pro-apoptotic protein of Bcl-2 family) were analyzed for interaction with Orf C via immunoprecipitation. Mitochondrial lysates were prepared using the MitoProfile® benchtop mitochondrial isolation kit for cultured cells (Mitosciences®) as previously described by transfecting HeLa cells with pKH3-Orf C plasmid and resuspending the pellet in RIPA buffer (Radioimmunoprecipitation assay buffer ; 150 mM NaCl, 1 % NP-40, 0.5% sodium deoxycholate, 0.1% SDS, 50 mM Tris (pH 8.0), with proteinase inhibitors - 10 µL/mL) (200 µL). Samples were incubated at 4°C for one hour with rotation. The cell suspension was centrifuged at 14,000 rpm for 15 minutes at 4°C and the supernatant was placed in a new microcentrifuge tube and placed on ice. Protein concentrations were determined using the previously described Micro BCA™ protein assay kit (Thermoscientific®).

Protein G-Sepharose™ (GE Healthcare) (50 µL) was added to 500 µg protein. IP buffer was added to bring final volume to one mL and microcentrifuge tube was rotated overnight at 4°C. Solution was centrifuged at 14,000 rpm for 20 minutes at 4°C and

supernatant was transferred to a new microcentrifuge tube. Mouse anti-ANT mAb (Mitosciences®, 10 µg/ml) was added and each tube was rotated for 90 minutes at 4°C. Protein G-Sepharose™ (30 µL) was added to each tube and incubated overnight at 4°C with rotation.

The following day the tubes were pulse-centrifuged (14,000 rpm) for ten seconds, tubes were rotated and pulse-centrifuged (14,000 rpm) again. Supernatant was saved as the unbound fraction from the immunoprecipitation. RIPA buffer (one mL) was added to the pellet and suspension was rotated for 20 minutes at 4°C. Pulse centrifugation was repeated (ten seconds). RIPA buffer (one mL) wash was performed two times with two 20 minute rotations at 4°C, followed by pulse centrifugation as described above repeated twice. Supernatant was carefully removed. Samples were pelleted by centrifugation to remove the last traces of supernatant.

NuPage® SDS-PAGE loading buffer (20 µL) (Invitrogen™) was added to pellets and samples were heated at 95°C for three minutes. Beads were pelleted by centrifugation (14,000 rpm for one minute) and supernatants were collected and loaded onto a Nu-PAGE® Bis-Tris 12% acrylamide gel with MES buffer and 0.5 mL Nu-PAGE® antioxidant, and subjected to electrophoresis at 200 V for 50 minutes. Proteins were then transferred onto an Immobilon™ transfer membrane (Millipore™) as described above. Membranes were blocked with 1% serum albumin (BSA) (used specifically for ANT antibody) and incubated membrane for 30 minutes at room temperature.

We next added anti-HA antibody (12CA5, 1:1000) diluted in 1% BSA and incubated membrane at 4°C overnight. Membrane was washed with western wash buffer three times for ten minutes each and incubated with secondary antibody (Anti-mouse IgG peroxidase, 1:2000, diluted in 1% BSA) for one hour at room temperature. Following this incubation period, the membrane was washed with western wash buffer three times for ten minutes each and developed in TMB substrate (KPL™) as previously described.

Bax – Orf-C interaction was investigated by transfecting HeLa cells with pKH3-Orf C and performing mitochondrial isolation followed by immunoprecipitation as described above, with the exception that Bax antibody (Cell Signaling Technology™, 1:1000) was used and the membrane was blocked using blotto instead of the 1% BSA solution. HA-tagged Orf C was again detected with anti-HA antibody (12CA5, 1:1000).

AIF (Apoptosis-inducing factor) antibody (Cell Signaling Technology®, #4642) was used to identify interactions between Orf C and AIF. NIH-3T3 and MCA-205 cell lines (2×10^6 cells in 100 mm tissue culture plates) were infected with either Lenti Orf C or Lenti empty vector virus (MOI = 5, incubated for 72 hours). Cells were harvested and cell fractions were isolated as previously described using the MitoProfile® benchtop mitochondrial isolation kit for cultured cells (Mitosciences®). Mitochondrial fractions were lysed using Chaps® Cell Extract Buffer as previously described, and nuclear fractions were washed with Reagent B (MitoProfile® benchtop mitochondrial isolation kit for cultured cells; Mitosciences®) and lysed with Dignam C buffer as previously described. Protein concentrations were determined via the Micro BCA™ protein assay kit (Thermoscientific®) as previously described. Samples were loaded onto a Nu-PAGE® Bis-Tris 4-12% acrylamide gel with MES buffer and 0.5 mL Nu-PAGE®

antioxidant, and run at 200 V constant for 50 minutes. Staurosporine (5 μ M) treated NIH-3T3 cells (cytosolic fraction) were used as a positive apoptosis control. Proteins were transferred to an Immobilon™ transfer membrane (Millipore™) and run at 150 mAmps constant for two hours. Membrane was washed in TBS buffer (five minutes) and incubated with blotto at room temperature for 30 minutes. Membrane was washed again with TBS buffer (three times, five minutes each) and primary AIF antibody (Cell Signaling technology®) was diluted in primary antibody dilution buffer (1:1000) and allowed to incubate with membrane overnight with rocking at 4°C.

Twenty-four hours later the membrane was washed with TBS (three times, five minutes each) and secondary antibody (Anti-Rb IgG HRP-linked, 1:2000) was applied and incubated at room temperature for 90 minutes. Membrane was then processed as previously described and developed with TMB western blot kit (KPL™).

The preceding experiment was repeated twice using the same procedure but by transfecting either NIH-3T3 or HeLa cells with pKH3/pKH3-Orf C. For each transfection reaction we used 3×10^6 cells per 100 mm tissue culture plate (4 plates total, performed in duplicate to maximize cell products), incubated 24 hours until cells were approximately 60-80% confluent, and then performed the transfections. We combined 40 μ L FuGene® HD to 500 μ L Opti-MEM in polystyrene tubes and incubated this mixture for five minutes at room temperature. Ten μ g DNA (pKH3 or pKH3-Orf C) was added to the Fu-Gene®/Opti-MEM mixture and incubated it for 15 minutes at room temperature, and then layered onto the NIH-3T3 or HeLa cells. Cells were incubated for 48 hours at 37°C and harvested using the procedure described in the preceding paragraphs.

Proteinase K digestion. To more accurately determine the submitochondrial location of Orf C, a proteinase K digestion was performed on intact mitochondria isolated from HeLa cells transfected with pKH3/pKH3-Orf C as described above. The mitochondria were isolated as previously described using the MitoProfile® benchtop mitochondrial isolation kit for cultured cells (Mitosciences®), with the exception that the mitochondrial pellet was left intact. Mitochondria were then treated with proteinase K (0.2 µg) for 15 or 30 minutes, with a non-treated control sample and a mitochondrial sample lysed with RIPA buffer included for comparison. Samples were placed at 4°C with rotation for one hour, and then centrifuged for 15 minutes at 14,000 rpm. Protein concentrations were determined via the Micro BCA™ protein assay kit (Thermoscientific®) as previously described.

Protein samples (20 µg) were heated to 70°C for ten minutes and centrifuged at 14,000 rpm for 1 minute. Samples were then loaded onto a Nu-PAGE® Bis-Tris 12% acrylamide gel with MES buffer and 0.5 mL Nu-PAGE® antioxidant, and run at 200 V constant for 60 minutes. Proteins were transferred to an Immobilon™ transfer membrane (Millipore™) and run at 150 mAmps constant for four hours. The membrane was rinsed with TBS wash for five minutes and incubated in blotto at room temperature for one hour. Membrane was again washed with TBS (three times for five minutes each) and the primary antibody (XHA (12CA5) 1:1000) was applied. Membrane was incubated overnight at 4°C with rocking. Twenty-four hours later the membrane was washed with TBS (three times, five minutes each) and secondary antibody (G x M IgG, HRP-linked, 3:5000) was applied and incubated at room temperature for 90 minutes. Membrane was

processed as previously described and developed with TMB western blot kit (KPL™). The same membrane was re-probed using a Bcl-2 monoclonal antibody (1:1000) as a control, with an appropriate secondary antibody (anti-Rb IgG HRP, 1:2000) applied using the previously outlined procedure.

Results

AIM 1. To construct a recombinant lentivirus expressing WDSV Orf C and assess its affect on cell growth.

Production of recombinant WDSV Orf C lentivirus.

Previous experiments assessing the in vitro affects of Orf C utilized standard transient transfections with pKH3-Orf C. To further characterize WDSV Orf C a more efficient delivery system was desired to maximize the effects of Orf C. We chose to use a recombinant Lentivirus system because we anticipated this expression system would be more efficient at introducing Orf C into various target cells. Another advantage of this system is that the Orf C-expressing recombinant lentivirus is self inactivating, which is a necessary feature for future in vivo virus experiments. Individual plasmids physically separate the *env*, *pol*, and *gag-pro* sequences required for viral replication. By using a replication incompetent virus for the in vivo studies we could ensure that the viral effects were limited to the target cells (specifically tumor cells), and eliminated the confounding results associated with systemic viral infections.

A recombinant WDSV Orf C lentivirus vector was constructed by cloning the *orf c* open reading frame into the pLVX-Puro vector. The Orf C lentivirus and the empty vector lentivirus were pseudotyped with either vesicular stomatitis virus glycoprotein G (VSV-G) or a mouse/rat ecotropic retrovirus glycoprotein. By using the ecotropic virus we added an additional biosafety precaution as this virus will only infect mouse or rat cells. In contrast, the VSV-G virus infects multiple cells types, including human cells.

Our initial virus production using the Lenti-X™ HT Packaging System produced virus of low concentration, with the highest initial titers of VSV-G Lenti Orf C virus reaching 1×10^5 cfu/mL. We ultracentrifuged the virus to obtain a more concentrated virus sample and were able to increase the concentration of the VSV-G Lenti Orf C virus to 2.1×10^6 cfu/mL. The highest titers of ecotropic Lenti Orf C were 1×10^6 cfu/mL; however, most were significantly lower.

Similar challenges were encountered when producing both VSV-G Lenti empty vector and ecotropic Lenti empty vector viruses, with the highest obtained titers reaching 1×10^7 cfu/mL and 1×10^5 cfu/mL, respectively. We investigated potential factors contributing to our low virus levels, including effects of freezing and time from transfection to virus harvest. There was no appreciable concentration difference in virus that had been frozen at -80°C versus virus placed on ice and immediately titrated (6×10^4 cfu/mL, 7×10^4 cfu/mL, respectively). Since we harvested our virus 48 hours post-transfection we examined additional time points to determine if increased virus concentrations occurred outside of the recommended 48 hours. The results examining virus harvested at 24, 48, and 72 hours post-transfection showed a slightly higher virus

concentration as time progressed (1×10^4 cfu/mL, 5×10^4 cfu/mL, and 1×10^5 cfu/ml, respectively).

The highest virus concentrations were obtained using ultracentrifugation following virus production. We employed this technique on numerous occasions to enhance virus concentrations to levels high enough to effectively perform our in vitro experiments.

Orf C-expressing lentivirus reduces cell viability

Previous studies confirmed WDSV Orf C expression in regressing tumors by terminal deoxynucleotidyl transferase biotin-dUTP nick end labeling (TUNEL) demonstrated tumor cells undergoing apoptosis (Rovnak et al., 2007; Nudson et al., 2003; Rovnak and Quackenbush, 2010). When Orf C was overexpressed in cultured cells mitochondrial function was altered and apoptosis was induced (Nudson et al., 2003). These studies suggested that Orf C may function as an oncolytic protein.

To evaluate the potential of Lenti Orf C virus as an oncolytic therapeutic, we used a cell proliferation assay to screen various cell lines to evaluate Orf C's effect on cell viability. Following infection of 4T1 (mouse mammary tumor), MCA-205 (mouse sarcoma tumor) and NIH-3T3 (mouse fibroblast) cells with Lenti Orf C virus or Lenti empty vector control virus, cell viability was measured with Cell Titer 96[®] AQueous One solution. Our goal was to find a mouse tumor cell line that consistently exhibited apoptosis in association with Lenti Orf C virus infection for use in future in vitro and in vivo studies assessing the oncolytic potential of Orf C.

To determine the ideal concentration of 4T1 cells to plate in a 96-well plate for the cell viability assays, we performed a pilot experiment. We plated varying numbers of cells with the goal of assessing cell viability over a five day period. The cell concentrations used ranged from 7×10^3 cells/well to 2.8×10^5 cells/well. The 4T1 cells demonstrated very rapid growth with the highest cell concentration (2.8×10^5 cells/well) showing 100% confluency within 24 hours, and the lowest cell concentration (7×10^3 cells/well) was 100% confluent at four days after plating the cells.

We next established a growth curve for 4T1 cells using 2.5×10^3 cells/well in a 96 well plate, measuring cell viability (without virus effects) over a four day period (**Figure 1**). The purpose of this experiment was to determine the optimal time frame for cell growth following various experimental manipulations. 4T1 cell growth rate was maximal between days two to four; therefore we concluded that cell viability should be assessed between 48-72 hours post cell plating – within the time period of maximal cell growth, but prior to cell confluency and overgrowth. We also determined the optimal cell concentration for in vitro experiments in a 96 well plate was 2.5×10^3 cells/well, as this yielded a cell population that did not reach confluency within the 72 hour experimental parameters.

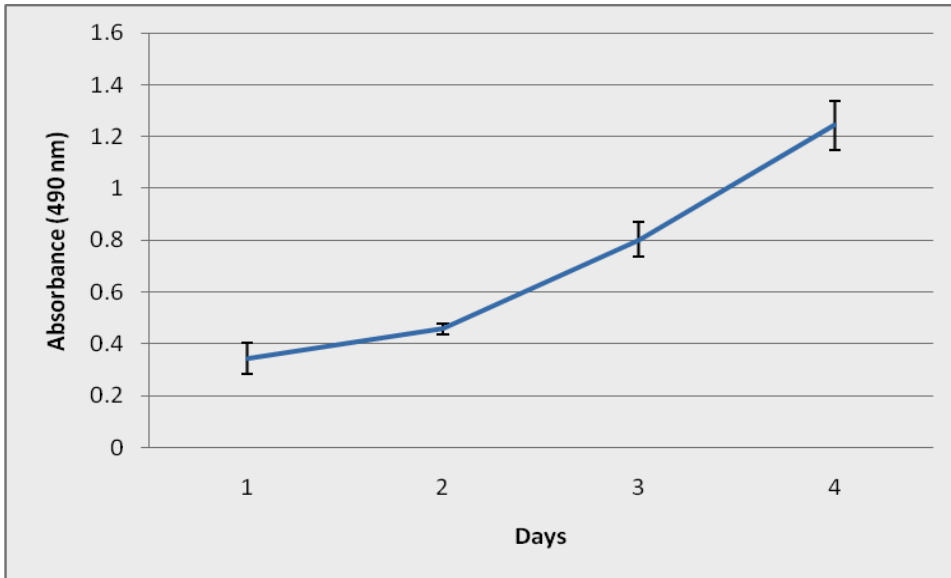


Figure 1. Growth curve of 4T1 cells. 2.5×10^3 cells per well were plated and cell viability measured by MTS assay. The mean OD_{490} readings from six replicate wells was determined for each time point.

Once we established an optimal cell concentration for use in the 96 well plates, we proceeded with the cell viability analysis in order to screen various cell lines for use in our in vitro experiments. We first used the 4T1 mouse mammary tumor cell line and infected cells with either Lenti Orf C virus (VSV-G) or Lenti empty vector virus (VSV-G) (n=5) with a multiplicity of infection (MOI) of 1.5. Cell viability was analyzed at 24, 72, and 96 hours post-infection with the CellTiter96® Aqueous One Solution Cell Proliferation Assay (MTS assay). No difference in cell viability was observed between the experimental and control groups (**Figure 2**).

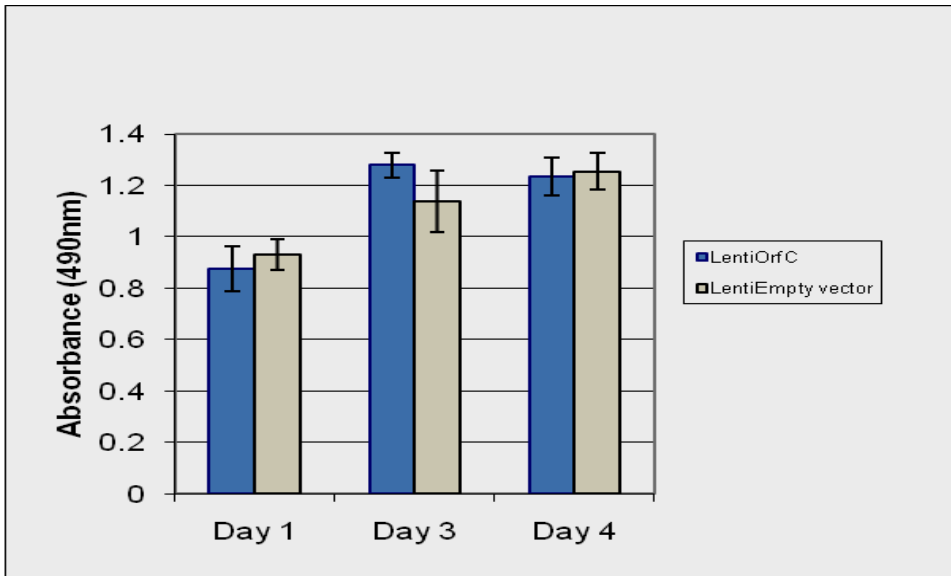


Figure 2. No significant reduction of 4T1 cells following infection with Lenti Orf C virus (MOI=1.5). 3.5×10^3 cells per well were plated and cell viability measured by MTS assay. The mean (OD_{490}) readings from five replicate wells were determined for each timepoint.

Since no observable decrease in cell viability was observed with Lenti Orf C infection, we surmised we needed to increase our virus concentration. Given that our virus is replication incompetent, we rely solely on individual cells being infected, and would not see virus spread throughout the culture. This virus safety feature may necessitate the use of slightly higher virus concentrations than initially anticipated.

We therefore repeated this experiment with increased MOI of 5, 10, and 100. A significant decrease in cell viability was observed at MOI=100 ($P < 0.00006$), with the percent of viable cells decreased to 45% in comparison to the uninfected control cells (**Figure 3**). However, when we repeated this experiment using appropriate Lenti empty vector controls (MOI=100), the same decrease in cell viability was observed in our Lenti empty vector control samples (data not shown). We concluded from these experiments

that at the high virus concentration of MOI=100, cell viability decreases independently of Orf C effects.

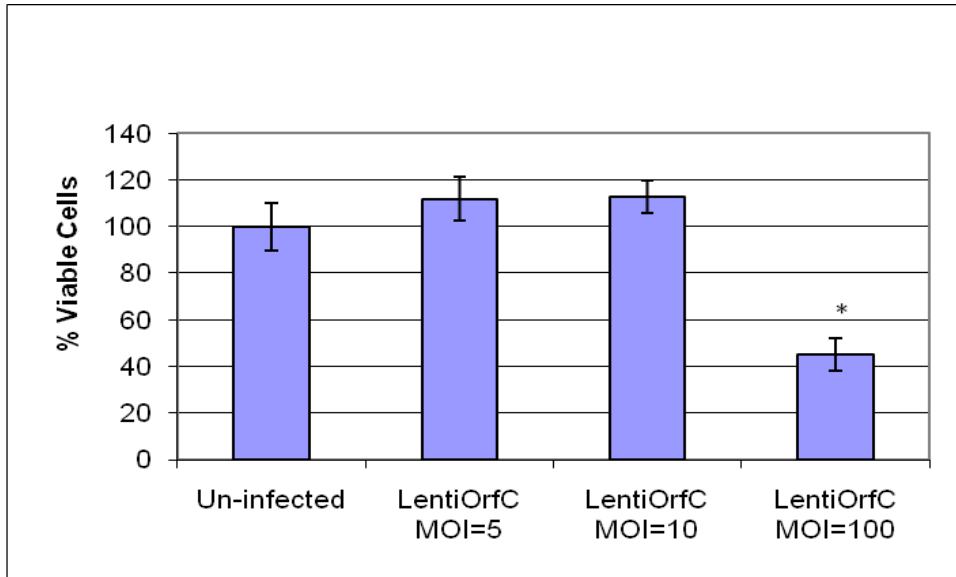


Figure 3. 4T1 cells infected with Lenti Orf C virus show a significant reduction at MOI=100. 2.5×10^3 cells per well were plated and cell viability measured by MTS assay three days post infection. The mean \pm standard deviation of OD₄₉₀ readings from replicates of six wells (Lenti Orf C, MOI=100, n=3) was determined and normalized to % viability.

To control for interassay differences with the two viruses, we repeated the cell viability experiment using 4T1 cells infected with Lenti Orf C and Lenti empty vector viruses at a MOI of 1, 5, or 10. A decrease in cell viability was observed in cells infected with Lenti Orf C virus at a MOI of 5 in comparison to the Lenti empty vector virus ($P < 0.003$) (**Figure 4**), with the percent of viable cells decreased to 72% of the Lenti empty vector infected control cells. However, this decrease in cell viability was not present at a MOI of 10 (data not shown). The Lenti empty vector virus did not have an effect on viability when compared to cells that were uninfected.

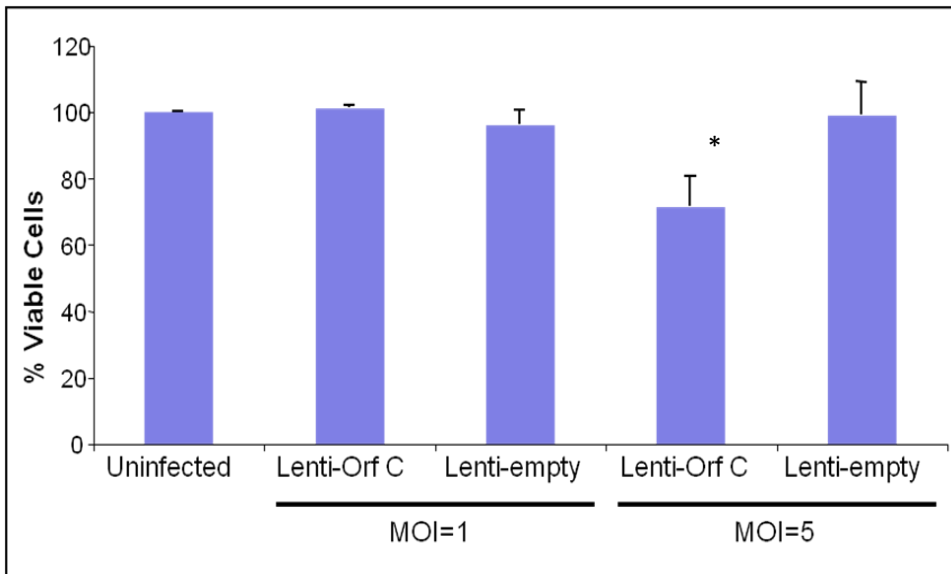


Figure 4. 4T1 cells infected with Lenti Orf C virus show a significant reduction at MOI=5. 2.5×10^3 cells per well were plated and cell viability measured by MTS assay three days post infection. The mean \pm standard deviation of OD₄₉₀ readings from replicates of three wells was determined and normalized to % viability.

The results from Figure 4 were promising as we did observe a significant decrease in viability of Orf C-expressing 4T1 cells at a MOI=5. However, the failure to significantly reduce cell viability in Orf C-expressing 4T1 cells at a MOI=10 led us to conclude that we should concurrently experiment with a non-tumor cell line as a control. We used NIH-3T3 cells, a mouse fibroblast cell line, as a non-tumor cell to control for any anti-apoptotic aberrations that may be present in the 4T1 cell line.

We infected both 4T1 and NIH-3T3 cells using a MOI of 1, 5, or 10 and results were analyzed 48 hours post-infection with the CellTiter Blue® MTS assay. This alternative assay was used for this experiment based on its ability to be used in conjunction with the Apo-One® Homogenous Caspase 3/7 assay (Promega™) (no results obtained). The results from this viability experiment show a trend towards decreasing

cell viability with increasing virus concentration in both 4T1 and NIH-3T3 cells.

However, a significant decrease was only observed in the NIH-3T3 cell line at MOI's of 5 and 10 ($p < 0.035$) (**Figure 5**), with the percent of viable cells decreased to 59% and 65% in comparison to the Lenti empty vector control cells, respectively.

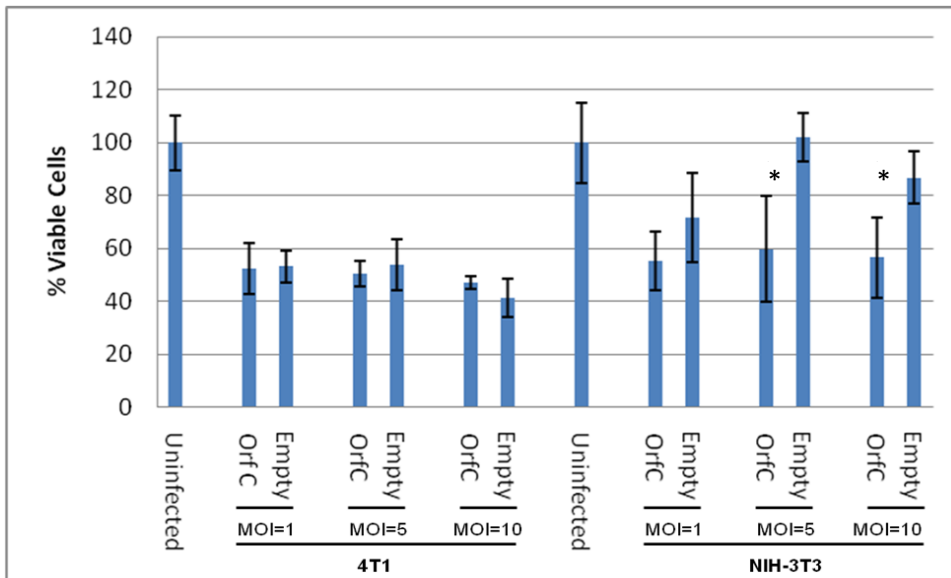


Figure 5. NIH-3T3 cells infected with Lenti Orf C virus show a significant reduction at a MOI of 5 and 10. 2.5×10^3 cells per well were plated and cell viability measured by MTS assay (CellTiter Blue®) two days post infection. The mean \pm standard deviation of $OD_{530(20)Ex/590(20)Em}$ readings from replicates of six wells was determined and normalized to % viability.

We repeated the experiment from Figure 5 and included the additional time points of 24 and 72 hours post-infection. The 24 and 72 hour time points showed no significant difference in cell viability between the Lenti Orf C and Lenti empty vector virus infected 4T1 or NIH-3T3 cells (data not shown). However, at 48 hours post-infection, the NIH-3T3 cells showed a significant decrease in viability at MOIs of 1 ($P < 0.004$) and 5 ($P < 0.012$), with the percent of viable cells decreased to 88% and 80%, respectively, in

comparison to the Lenti empty vector control cells. A decreased viability was also present at a MOI of 10, however the decrease was not significant, possibly related to our small sample size. 4T1 cells exhibited no decrease in cell viability with Lenti Orf C infection (**Figure 6**).

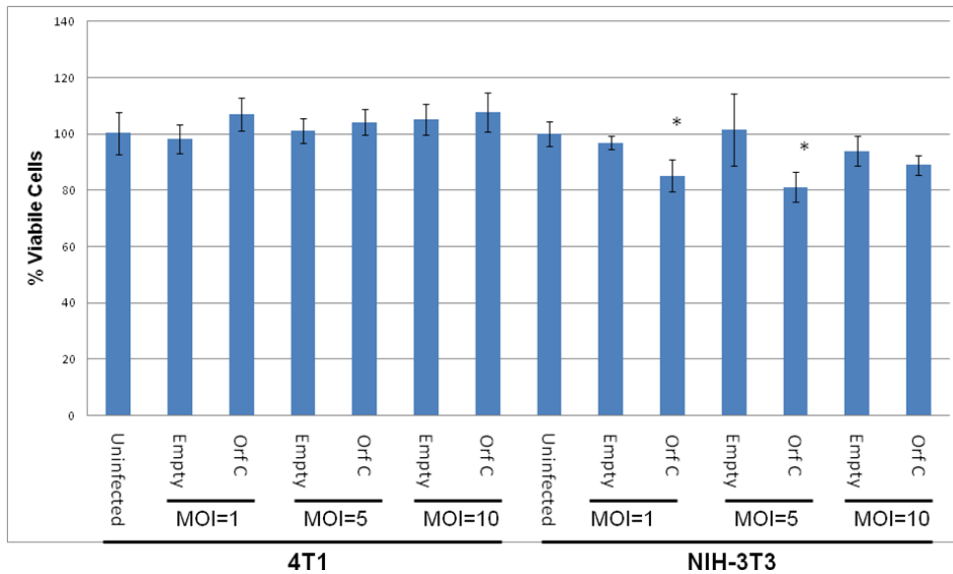


Figure 6. NIH-3T3 cells infected with Lenti Orf C virus show a significant reduction at a MOI of 1 and 5. 2.5×10^3 cells per well were plated and cell viability measured by MTS assay two days post infection. The mean \pm standard deviation of OD₄₉₀ readings from replicates of six wells was determined and normalized to % viability.

Our results from Figures 4-6 demonstrate the difficulties we had in using the 4T1 cell line for our viability assays. In comparison to the NIH-3T3 cells, 4T1 Orf C-expressing cells did not consistently decrease cell viability. We concluded that based on these results, the 4T1 cell line was not amenable to the in vitro studies we needed to conduct to assess the apoptotic ability of Lenti Orf C virus. The rapid growth rate of 4T1 cells is likely the major characteristic that made them resistant to exhibiting consistent and observable Orf C-induced apoptosis.

We replaced the 4T1 cells with an alternative mouse tumor cell, MCA-205. MCA-205 is a mouse sarcoma cell line that has been well-characterized in vitro and in vivo. We repeated cell viability experiments using NIH-3T3 and MCA-205 cells infected at a MOI of 10 or 20, and examined time points at 24, 48, and 72 hours post-infection (**Figures 7-9**). A significant decrease in cell viability was observed 24 hours post-infection at a MOI of 10 in both MCA-205 ($P<0.0005$) and NIH-3T3 cells ($P<0.03$). At a MOI of 10, viability of MCA-205 cells expressing Orf C decreased to 80% in comparison to the Lenti empty vector controls. The NIH-3T3 Orf C-expressing cell viability decreased to 95% in comparison to the Lenti empty vector controls. There was also a mean decrease in cell viability at a MOI of 20 in both cell lines that was not statistically significant (**Figure 7**).

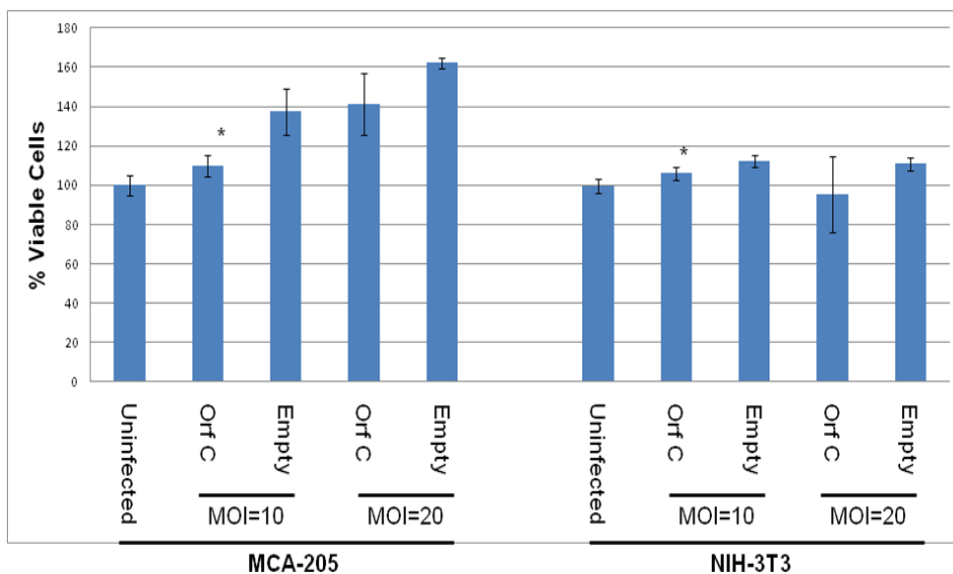


Figure 7. MCA-205 and NIH-3T3 cells infected with Lenti Orf C virus demonstrate significant reduction at a MOI of 10. 2.5×10^3 cells per well were plated and cell viability measured by MTS assay one day post infection. The mean \pm standard deviation of OD₄₉₀ readings from replicates of six wells was determined and normalized to % viability.

At 48 hours post-infection a significant decrease in cell viability was observed at a MOI of 10 in both MCA-205 ($P<0.00006$) and NIH-3T3 cells ($P<0.00003$) and a MOI of 20 in MCA-205 ($P<0.0002$) and NIH-3T3 ($P<0.04$) cells. The NIH-3T3 cells showed the most significant cell viability decrease at a MOI of 20 two days post-infection, with a cell viability of 45% in comparison to the cells infected with Lenti empty vector virus. The MCA-205 cells also showed a significant cell viability decrease at a MOI of 20, with a cell viability of 55% in comparison to Lenti empty vector virus (**Figure 8**).

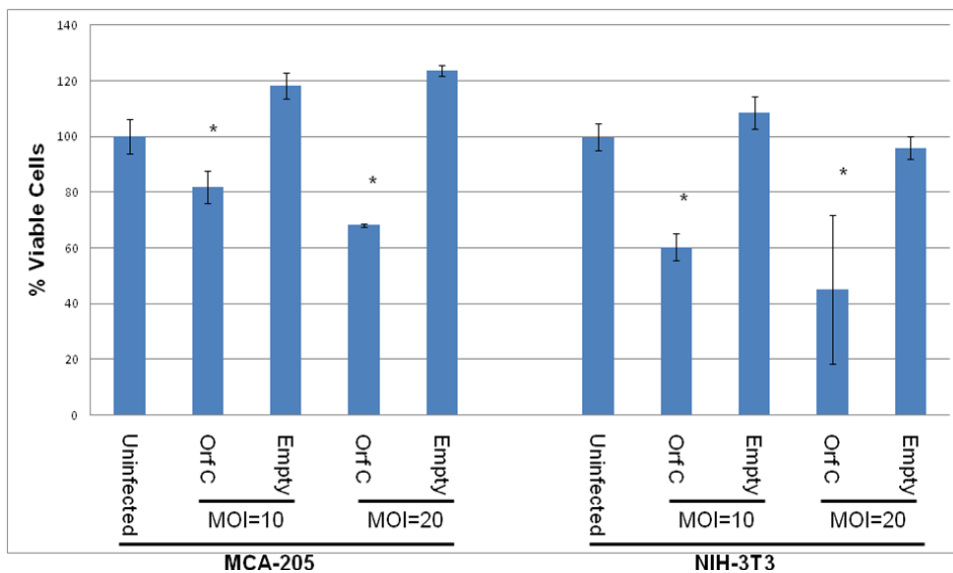


Figure 8. MCA-205 and NIH-3T3 cells infected with Lenti Orf C virus demonstrate significant reduction at a MOI of 10 and 20. 2.5×10^3 cells per well were plated and cell viability measured by MTS assay two days post infection. The mean \pm standard deviation of OD_{490} readings from replicates of three-six wells (MOI=10, n=6; MOI=20, n=3) was determined and normalized to % viability.

A significant decrease in cell viability was observed 72 hours post-infection at a MOI of 10 in NIH-3T3 cells ($P<0.006$) and a MOI of 20 in MCA-205 ($P<0.03$) and NIH-3T3 ($P<0.007$) cells. The NIH-3T3 cells again showed the most significant decrease in cell viability at a MOI of 20 three days post-infection, with a cell viability of

41% in comparison to the cells infected with Lenti empty vector virus. The MCA-205 cells demonstrated a cell viability of 88% at a MOI of 20 in comparison to Lenti empty vector virus infected cells (**Figure 9**). The results from Figures 7-9 led us to conclude that the most significant decreases in cell viability occurred 48 hours post infection, and that these decreases, while present in both the MCA-205 and NIH-3T3 cell lines, were most pronounced in the NIH-3T3 cells. We also concluded that given these results, the MCA-205 cells would serve as an appropriate in vitro model of Orf C-induced apoptosis.

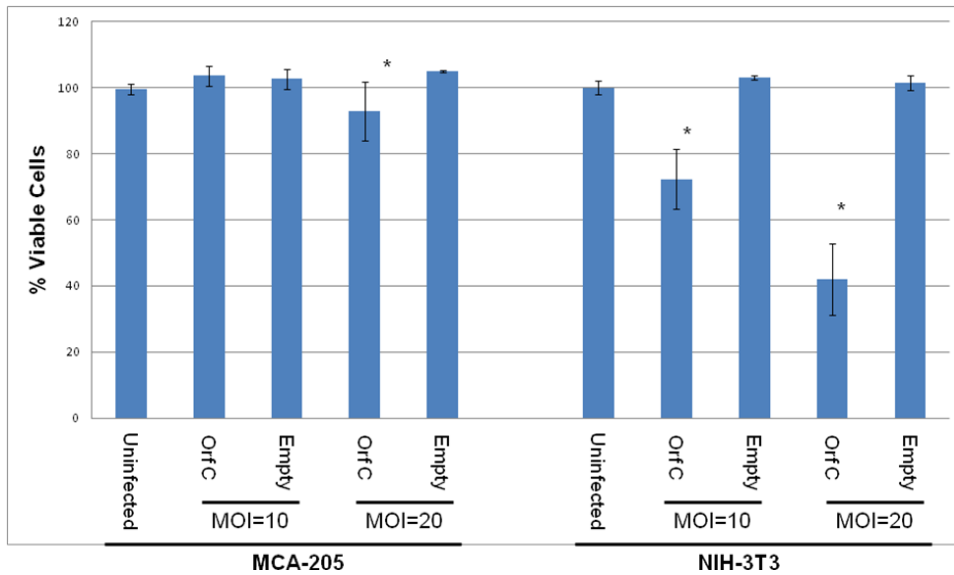


Figure 9. NIH-3T3 (MOI 10 and 20) and MCA-205 (MOI=20) cells infected with Lenti Orf C virus demonstrate significant reduction of viable cells. 2.5×10^3 cells per well were plated and cell viability measured by MTS assay three days post infection. The mean \pm standard deviation of OD₄₉₀ readings from replicates of six wells was determined and normalized to % viability.

AIM 2. To determine the subcellular localization of the lentivirus expressed Orf C.

Orf C is expressed in mitochondrial, nuclear, and cytosolic cell fractions

Given previous research by Nudson et al. (2003) we believed Orf C would be expressed in the cell mitochondria. We transfected HeLa cells with pKH3-Orf C and examined the mitochondrial and cytosolic cell fractions for Orf C expression. We found that Orf C was expressed in both the mitochondrial and cytosolic cell fractions, indicating that Orf C is not exclusively located in the mitochondria (**Figure 10**).

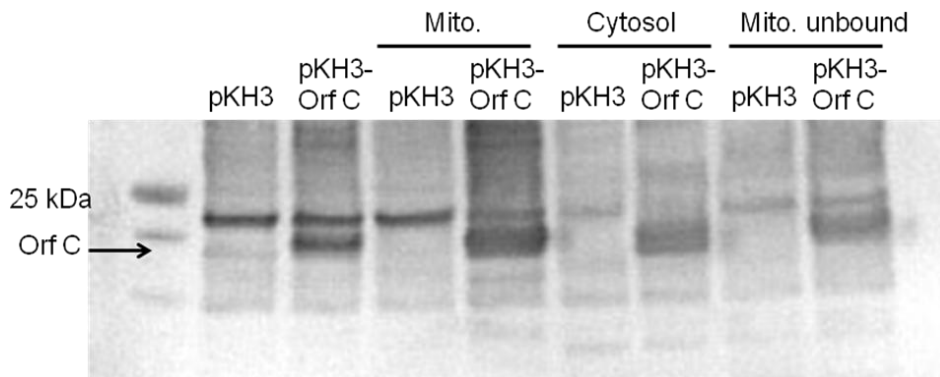


Figure 10. WDSV Orf C is present in mitochondrial and cytosolic cell fractions of HeLa cells transfected with pKH3-Orf C. Enriched mitochondrial and cytosolic cell lysates were immunoprecipitated and HA-tagged Orf C was detected with anti-HA antibody (12CA5). Lysates from HeLa cells transfected with Orf C (pKH3-Orf C) or control vector (pKH3) serve as controls.

Previous unpublished results from the Quackenbush laboratory (Hronek, Rovnak and Quackenbush, unpublished) indicated that WDSV Orf C was present in nuclear extracts from tumors. To examine potential Orf C expression in the cell nuclei and to confirm previous observations, we transfected HeLa cells and isolated the mitochondrial, nuclear, and cytosolic cell fractions. We observed robust Orf C expression in all cell fractions, including the nuclear extract (**Figure 11**).

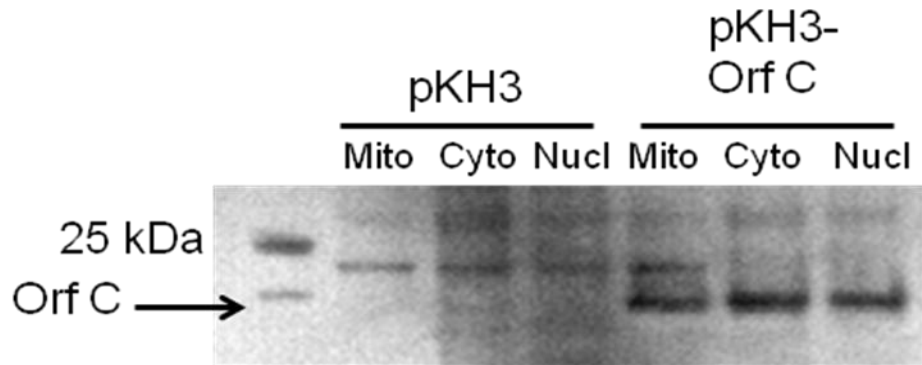


Figure 11. WDSV Orf C is present in mitochondrial, cytosolic, and nuclear cell fractions of HeLa cells transfected with pKH3-Orf C. Enriched mitochondrial (mito), cytosolic (cyto), and nuclear (nucl) cell lysates were analyzed via Western blot and HA-tagged Orf C was detected with monoclonal anti-HA antibody (12CA5).

To further examine this intranuclear location of Orf C, we used 4T1 and HeLa cells infected with Lenti Orf C virus (estimated MOI=0.006) and analyzed mitochondrial, nuclear, and cytosolic cell fractions. Orf C was expressed in all cell fractions, however the nuclear cell fraction showed the most robust Orf C expression (**Figure 12**).

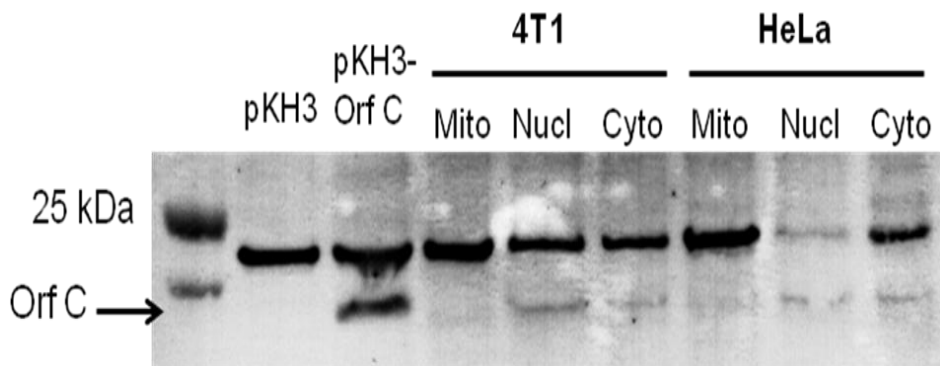


Figure 12. WDSV Orf C is expressed in mitochondria, nuclear, and cytosolic fractions. 4T1 and HeLa cells were infected with Lenti Orf C virus (est. MOI=0.006) and separated into mitochondrial (mito), nuclear, (nucl), and cytosolic (cyto) fractions 48 hrs post infection and analyzed by western blot. HA-tagged Orf C was detected with anti-HA (12CA5) monoclonal antibody. Lysates from 4T1 cells transfected with Orf C (pKH3-Orf C) or control vector (pKH3) serve as controls.

Based on the results of Figures 11-12 we concluded that Orf C was expressed in mitochondrial, nuclear, and cytosolic cell fractions following transient transfection and Lenti Orf C virus infection. Although the results from the Lenti Orf C cell infections (**Figure 12**) showed the same localization pattern as the pKH3-Orf C transfections (**Figure 11**), the intensity of Orf C expression differed between the two experiments. The Lenti Orf C infection experiment showed that while Orf C continued to be expressed in all cell fractions, the nuclear cell fraction exhibited the most robust Orf C expression. The pKH3-Orf C transfection experiments showed relatively equal amounts of Orf C expression in the various cell fractions. This difference in Orf C expression intensity may suggest differences in subcellular localization that are dependent on the method of Orf C cellular introduction.

AIM 3. To determine the mechanism of Orf C-induced apoptosis

Orf C-induced apoptosis functions via a caspase-independent pathway

To elucidate the underlying mechanism(s) of Orf C-induced apoptosis, we examined activated caspases 3, 6, 9, 12, and cleaved PARP following infection with Orf C. Activation of a specific caspase was identified by western blot analysis of its cleaved form. We used multiple cell lines for caspase analysis, including 4T1, MCA-205, and NIH-3T3 cells. Cells were infected with either Lenti Orf C or Lenti empty vector virus and harvested 48 hours post-infection.

We initially used IP buffer to lyse our cell samples and found one unique finding in that cleaved PARP was activated in all 4T1 cell samples (uninfected, Lenti empty vector infected, and Lenti Orf C infected) (data not shown). Activation of PARP in the 4T1 tumor cell line is not entirely unexpected. PARP is often activated in cancer cells as it facilitates DNA repair and promotes uncontrolled cell growth (Helleday et al., 2005).

Caspase-3 is an effector caspase, which is directly activated/cleaved by caspases 7, 8, 9, and 10 during caspase-dependent apoptosis (Salvesen and Riedl, 2008). Our results showed no evidence of activation of caspase 3 (**Figure 13**) or any of the other caspases we examined (data not shown) following infection with Lenti Orf C.

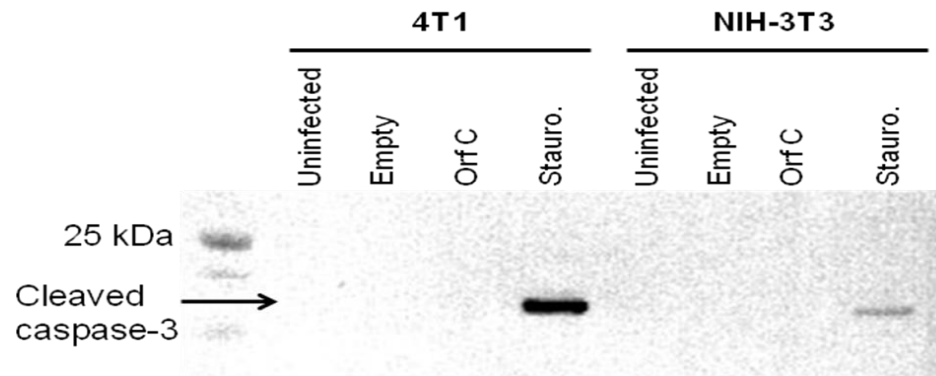


Figure 13. Cleaved caspase-3 is not detectable in Orf C expressing cells. 4T1 and NIH-3T3 cells were infected with Lenti Orf C (MOI=10) or Lenti empty vector control virus (Empty). Uninfected cells were used as a negative control and staurosporine (stauro.) treated cells (5 μ M) served as a positive apoptosis control. Cleaved caspase-3 Rabbit mAb (Asp175) (1:1000) was used to detect the cleaved caspase.

We repeated this experiment substituting Chaps® cell extract buffer for the IP buffer, as a reference was found suggesting this buffer is more appropriate for caspase activation analysis. Our results were the same – the examined caspases showed no

evidence of activation following infection with Lenti Orf C (data not shown). These results suggest that Orf C induces apoptosis via a caspase independent mechanism.

Orf C interacts with ANT and Bax

In our quest to identify a specific Orf C target in mitochondria and to further define the mechanism(s) of Orf C-induced apoptosis, we performed immunoprecipitation assays to assess Orf C interaction with apoptosis-specific proteins. Based on a previous study that showed alteration of the mitochondrial membrane potential and work by others demonstrating interaction of other viral proteins with components of the mitochondria permeability transition pore complex (PTPC), we first examined two components of the PTPC, VDAC and ANT (Nudson et al., 2003; Boya et al., 2001). Mitochondrial lysates harvested from HeLa cells transfected with pKH3 or pKH3-Orf C were immunoprecipitated using anti-VDAC and anti-ANT antibodies. We were able to detect Orf C interaction with the ANT antibody, but not VDAC antibody via co-IP (**Figure 14** and data not shown).

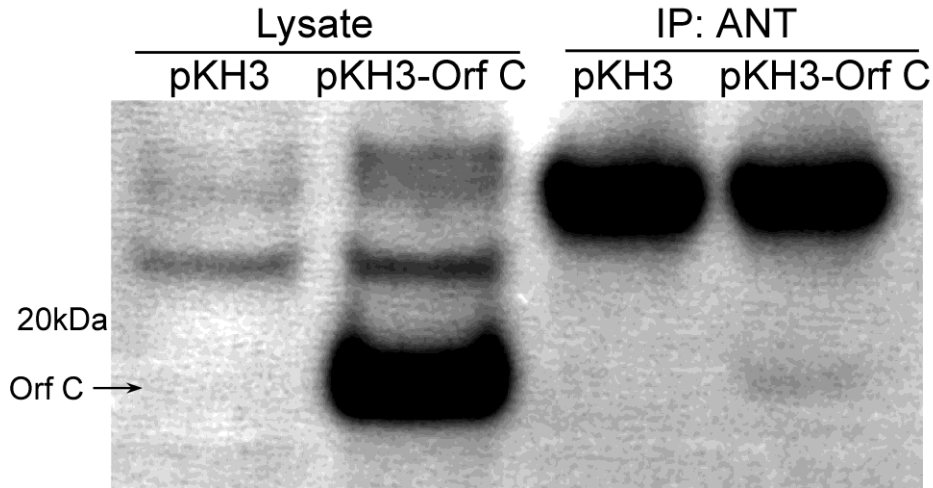


Figure 14. WDSV Orf C is present in a complex with adenine nucleotide translocase (ANT). Enriched mitochondrial lysates were immunoprecipitated with a mouse anti-ANT monoclonal antibody. HA-tagged Orf C was detected with anti-HA antibody (12CA5). Lysate represents 15% of the total amount used for immunoprecipitation.

We next examined possible interaction of Orf C with Bcl-2 and Bax as both are pro-apoptotic proteins. Bcl-2 is located in the outer mitochondrial (OM) membrane and Bax is a Bcl-2 family protein that mediates permeabilization of the OM membrane, inducing apoptosis via disruption of the OM membrane (Kroemer et al., 2007). In a similar fashion to the co-IP of Orf C with ANT antibody, a small amount of the expressed Orf C was co-IP with Bax (**Figure 15**), but not with Bcl-2. These data suggest that Orf C may be interacting with ANT and Bax, however the lack of a robust band indicates that this interaction may not be direct.

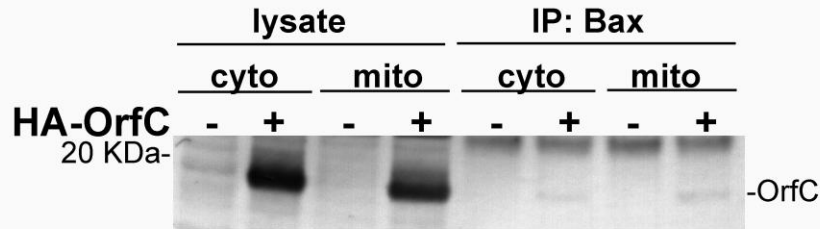


Figure 15. WDSV Orf C is present in a complex with Bax (Bcl-2 family) in the mitochondrial and cytosolic fractions. Enriched mitochondrial lysates were immunoprecipitated with a mouse anti-Bax monoclonal antibody. HA-tagged Orf C was detected with anti-HA antibody (12CA5).

Orf C localizes to the inner/inter-mitochondrial membrane space

To more definitively determine the submitochondrial localization of Orf C we purified mitochondria from Orf C expressing cells and from control cells. Mitochondrial samples were treated with proteinase K or control buffer. Treatment of mitochondria with proteinase K should digest proteins located in the OM membrane. Bcl-2, a known OM membrane protein, was used as a control and was not detected in the proteinase K treated samples. We found that Orf C expression remains intact with proteinase K treatment (**Figure 16**), indicating that Orf C is not located in the OM membrane but rather resides in either the inner mitochondrial membrane or the inter-mitochondrial membrane space. However, repeat experiments have shown some ambiguous results and further experiments are underway to clarify the association of Orf C with the outer mitochondrial membrane.

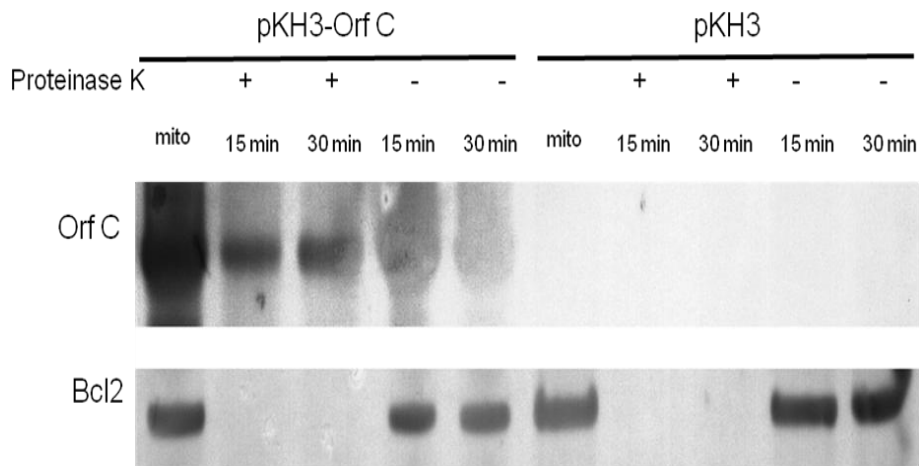


Figure 16. WDSV Orf C is not associated with the outer mitochondrial membrane. Mitochondria isolated from HeLa cells transfected with pKH3-Orf C or pKH3 control and treated with proteinase K for 15 or 30 minutes. Bcl-2 used as a control. Samples analyzed by western blot with anti-HA (12CA5) monoclonal antibody used to detect HA-tagged Orf C.

Interaction of Orf C with AIF

Our results indicate that Orf C appears to induce apoptosis via a caspase independent mechanism. Given the results of the proteinase K experiment, we were interested in the interaction of Orf C with AIF (apoptosis-inducing factor) since AIF is located in the inter-membrane space of the mitochondria. We were additionally interested in this protein given the robust expression of Orf C in the nucleus, and the tendency of AIF to translocate to the nucleus upon activation. We examined NIH-3T3 and MCA-205 cell fractions following Lenti Orf C and Lenti empty vector virus infection and found AIF expression in all cell fractions (mitochondrial, cytoplasmic, and nuclear) via western blot, with slightly more robust expression in the nuclear cell fraction of Lenti Orf C infected cells (**Figure 17**).

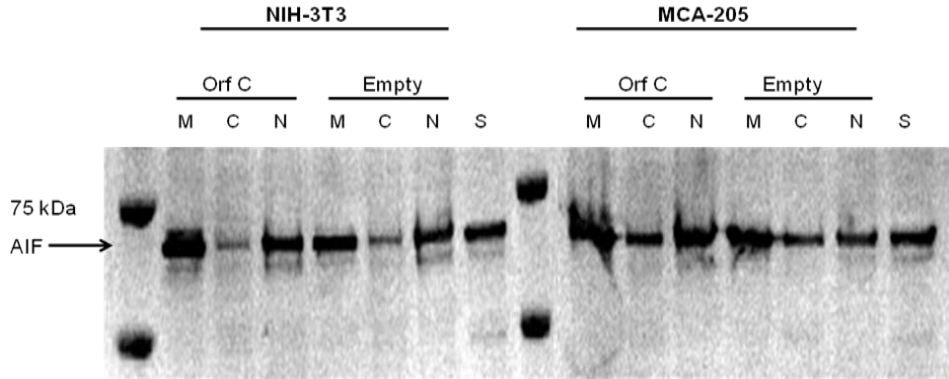


Figure 17. AIF is expressed in the mitochondria (M), cytosolic (C), and nuclear (N) cell fractions of NIH-3T3 and MCA-205 cells infected with Lenti Orf C or Lenti empty vector virus (MOI=5). NIH-3T3 treated with staurosporine (S) (5 μ M) used as a positive apoptosis control. Samples analyzed by western blot with anti-Rb IgG HRP-linked (1:2000) monoclonal antibody used to detect Anti-AIF Ab.

AIF expression was also demonstrated in all cell fractions following transfection of NIH-3T3 cells (**Figure 18**) and HeLa cells (**Figure 19**) with pKH3 or pKH3-Orf C. Expression of Orf C was confirmed in pKH3-Orf C transfected HeLa cells (**Figure 19**). Although AIF is expressed in all cell fractions, the most robust expressions were observed in the mitochondria and nuclear cell fractions.

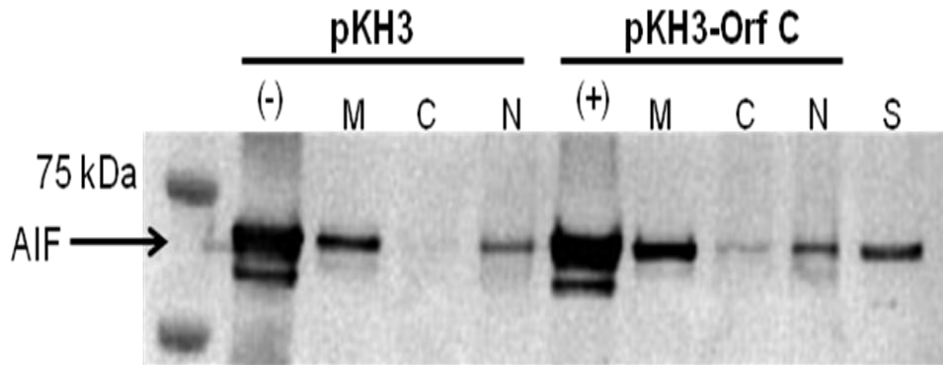


Figure 18. AIF is expressed in mitochondria (M), cytosolic (C), and nuclear (N) cell fractions of NIH-3T3 cells transfected with Orf C (PKH3-Orf C) or control vector (pKH3). NIH-3T3 treated with staurosporine (S) (5 μ M) used as a positive apoptosis control. Samples analyzed by western blot with anti-Rb IgG HRP-linked (1:2000) monoclonal antibody used to detect Anti-AIF Ab.

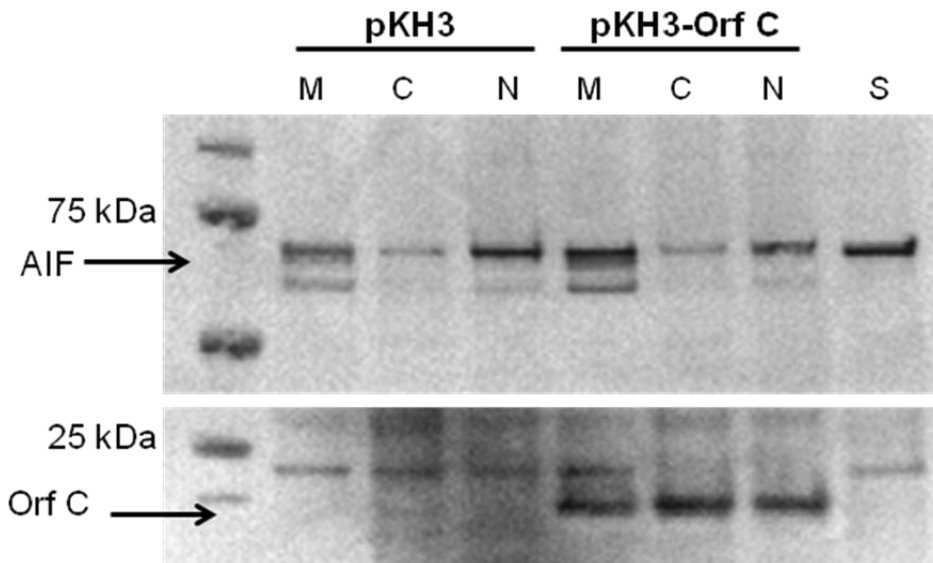


Figure 19. AIF is expressed in mitochondria (M), cytosolic (C), and nuclear (N) cell fractions of HeLa cells transfected with Orf C (PKH3-Orf C) or control vector (pKH3). NIH-3T3 treated with staurosporine (S) (5 μ M) used as a positive apoptosis control. Orf C expression confirmed (anti-HA (12CA5) monoclonal antibody). Samples analyzed by western blot with anti-Rb IgG HRP-linked (1:2000) monoclonal antibody used to detect Anti-AIF Ab.

These data suggest that AIF is being cleaved from its inter-mitochondrial membrane location and translocating to the nucleus. However, AIF activation does not appear to be limited to Orf C-expressing cells. Further studies are therefore needed to examine the exact nature of the relationship between Orf C and AIF.

Discussion

Recombinant Orf C lentivirus expression system

In fulfillment of specific AIM 1, we successfully created an Orf C-expressing lentivirus (Lenti Orf C) that was confirmed via DNA sequencing. This recombinant virus was created for two purposes. The first was to have a means of introducing Orf C into target cells with a high degree of efficiency. The second purpose was focused on its future in vivo use – this recombinant Orf C-expressing virus is replication incompetent as it lacks *gag*, *pol*, and *env*, which would be required for viral replication.

This characteristic of replication incompetency conveys several biosafety features. By using a replication incompetent virus for the in vivo studies we can ensure that the viral effects are limited to the target tumor cells and eliminate the risks associated with systemic viral infections. We further enhanced the safety of using this virus in research studies by producing an Ecotropic Lenti Orf C virus that is specific to mouse/rat cells. By using a virus with an ecotropic envelope we are ensuring that the virus will only infect mouse (or rat) cells, our model of interest, and not human cells.

We encountered difficulties in producing high virus titers with both the VSV-G and Ecotropic Lenti Orf C viruses. While we were able to obtain virus, the virus produced yielded consistently low virus titers. After several attempts at producing virus that resulted in low viral titers, we decided that we could enhance our virus titers by ultracentrifugation. This step increased our virus titers by approximately ten-fold, and became a necessary procedure following virus production. However, even with ultracentrifugation, our highest virus concentrations only reached levels of 10^7 cfu/mL (VSV-G) and 10^6 cfu/mL (Ecotropic). At these virus concentrations we were able to proceed with our in vitro experiments, but needed to continually grow virus throughout the series of thesis experiments as we needed relatively large virus volumes to conduct our experiments.

We investigated other potential causes of low virus levels. We examined virus titers from virus that had been frozen at -80°C and compared these titers to the same virus that was not frozen before use. No appreciable difference was observed indicating that freeze/thaw did not have a large effect on virus titers, at least after one freeze/thaw cycle. We also investigated harvesting viral supernatants outside of the 48 hour recommended time point post-transfection. We harvested the supernatants at an earlier time point (24 hours) and a later time point (72 hours) post-transfection. We did observe a slightly higher virus titration in association with the 72 hour time point in comparison to both the 24 and 48 hour time points (10^4 cfu/mL at 24 hours, 5×10^4 cfu/mL at 48 hours, and 10^5 cfu/mL at 72 hours). While this increase was not high enough to significantly benefit our in vitro experiments we did modify our virus harvest technique to delay collection until 48-72 hours post-transfection.

For future experimental in vivo use of the Lenti Orf C virus it would be beneficial to produce large amounts of virus and ultracentrifuge this virus. Resuspending the virus in relatively small amounts of buffer solution (1/1000th of original volume) will assist with producing virus titers with high concentrations to effectively complete the in vivo injections. Although challenging, the benefit of having a replication incompetent virus is necessary for future in vivo studies assessing the oncolytic potential of Lenti Orf C virus.

Orf C-expressing cells demonstrate decreased cell viability

To screen various cell lines for their potential use as an in vitro cell model of Orf C-induced apoptosis, we used a MTS cell proliferation assay to assess cell viability following Lenti Orf C and Lenti empty vector virus infections. We initially focused on the 4T1 mouse mammary tumor cell line for several reasons. Since this cell line is a mouse mammary tumor cell line, its use would transition well from in vitro to in vivo experimentation. Mouse mammary tumor cells are easily injected into the mammary fat pads of mice and following tumor growth, easily accessible for experimental manipulation. In addition, these cells have been extensively used at Colorado State University in various oncology studies and thus are well characterized. We know the tumor growth rate timeline from point of injection until potential ulceration and could plan an in vivo experiment around this known timeline.

Unfortunately the 4T1 cell line did not exhibit consistent decreases in cell viability following Lenti Orf C infection (Figures 2, 5, and 6). To determine if the resistance of 4T1 cells to Lenti Orf C-induced apoptosis was specific to this tumor cell

line, we refined our in vitro assay and analyzed an alternative non-tumor cell line in conjunction with the 4T1 cells. We used a mouse fibroblast cell line, NIH-3T3 cells, to control for any aberrations or apoptosis-resistant properties with the 4T1 tumor cell line and found that the NIH-3T3 cells exhibited significant decreases in cell viability that correlated with increasing Lenti Orf C virus concentrations (Figures 5-6). With the NIH-3T3 cell line we finally demonstrated that Lenti Orf C could induce significant reductions in cell viability.

There are likely several reasons the 4T1 cells failed to consistently exhibit Orf C-induced apoptosis in our studies. The most pronounced cause of apoptosis-resistance is most likely related to the very rapid growth rate of 4T1 cells. While the 4T1 cells showed minor decreases in viability in association with Lenti Orf C infection, these decreases were most often not significant and not consistently repeatable. We believe that while Orf C was inducing some degree of apoptosis in the 4T1 cell line, the rapid growth rate of these cells made any apoptosis-induced decreases difficult to detect with our MTS cell proliferation assays.

The lack of perceivable cell death in the 4T1 cells with Lenti Orf C infection led us to experiment with an alternative tumor cell line, MCA-205 cells, a mouse sarcoma cell line. We chose this cell line because similar to the 4T1 cells it had also been extensively used for oncology studies at CSU and was well characterized. We ran a series of cell viability experiments examining MCA-205 and NIH-3T3 cells infected with various virus concentrations and analyzed different time points post-infection. We observed that both the MCA-205 and NIH-3T3 cells showed significant decreases in cell

viability following Lenti Orf C virus infection (Figures 7-9), and there was a direct relationship between decreasing cell viability and increasing virus concentration.

These results indicate that the observed decreased viability with Lenti Orf C infection is solely attributable to Orf C, and serves as further evidence that Orf C induces apoptosis. In addition, this series of experiments using MCA-205 cells demonstrate that this tumor cell line shows consistent apoptosis when infected with Lenti Orf C virus and suggests the MCA-205 cells will serve as a suitable in vitro model (and potential in vivo model) of Orf C-induced apoptosis.

Orf C is expressed in mitochondrial, nuclear, and cytosolic cell fractions

In our quest to discover the mechanism(s) of Orf C-induced apoptosis, we needed to determine the intracellular target of Orf C. We initially determined the intracellular location of Orf C following transfection of HeLa cells. Previous studies had demonstrated Orf C expression in the cell mitochondria following cell transfections with pKH3-Orf C (Nudson et al., 2003). In addition to examining the mitochondrial cell fractions, we examined cytosolic and nuclear fractions for Orf C expression following pKH3-Orf C transfection of HeLa cells (Figures 10-11). Based on the previous results of Nudson et al. (2003), we expected to observe the most robust Orf C expression in the mitochondrial cell fraction. While we did observe Orf C expression in the mitochondria, the cytosolic and nuclear fractions also exhibited robust Orf C expression (Figure 11).

To determine if this subcellular localization pattern was demonstrable following infection with Lenti Orf C virus, we analyzed the mitochondrial, cytosolic, and nuclear

cell fractions of 4T1 and HeLa cells infected with Lenti Orf C virus. While Orf C continued to be expressed in all cell fractions following infection, our Lenti Orf C results differed from our pKH3-Orf C transfections in the intensity of Orf C expression. We found that following Lenti Orf C infection, Orf C expression was most robust in the nuclear extract (Figure 12). This difference in Orf C expression intensity may suggest differences in subcellular localization that are dependent on the method of Orf C cellular introduction. For example, in comparison to the pKH3-Orf C transient transfections, the use of a lentivirus introduction system may stimulate different pathways within the cell that localize Orf C to the nucleus. Another potential explanation for this difference in Orf C expression intensity may be related to the timing of experiments. Further studies examining subcellular Orf C localization along a defined timeline are warranted to determine if the sequence of events following Lenti Orf C infection affect the subcellular location of Orf C.

We believe this finding of nuclear localization of Orf C is significant in decoding the mechanism(s) of Orf C-induced apoptosis. Our findings of robust nuclear expression, coupled with the previous findings of mitochondrial expression, indicate that the mechanism of Orf C induced apoptosis may function at both the mitochondrial and the nuclear locations, and further studies are needed to determine which subcellular structure is targeted first by Orf C. We additionally would like to determine which potential pro-apoptotic proteins are targeted by Orf C in the mitochondria and nucleus.

Orf C-induced apoptosis functions via a caspase-independent pathway

In further efforts to elucidate the underlying mechanism(s) of Orf C-induced apoptosis, we focused on determining whether Orf-C induced apoptosis was occurring via a caspase-dependent or caspase-independent pathway. Orf C has previously been shown to be associated with a decrease in mitochondria-associated cytochrome c (Nudson et al., 2003). When cytochrome c is liberated from the mitochondrial membrane it will initiate a caspase-dependent apoptotic cascade by interacting with Apaf-1 (Apoptotic protease activating factor-1) to form the apoptosome, which in turn activates procaspase-9 (Yuan et al., 2010). Given this previous observation, we expected Orf C would initiate apoptosis via a caspase-dependent pathway, and that both caspases -9 and -3 would be activated in Orf C-expressing cells.

We examined a variety of caspases (3, 6, 9, 12, and cleaved PARP) and conducted experiments using multiple cell lines. Although we initially used IP buffer to lyse our cell samples, we moved to an alternative buffer (Chaps® cell extract buffer), upon recommendation from the manufacturer. Regardless of our experiment modifications and refinements, we were unable to show evidence of caspase activation following infection with Lenti Orf C (Figure 13).

Given the lack of caspase activation it appears that Orf C induces apoptosis in a caspase-independent manner. A variety of non-caspase cell proteases have been shown to cause apoptosis, such as AIF, endonuclease G (Endo-G), and OMI/HtrA2 (Omi stress-regulated endoprotease/high temperature requirement protein A2) (Bröker et al, 2005; Kroemer et al, 2007). The finding that Orf C appears to function in a caspase-

independent manner furthers our understanding of its basic mechanism of induced apoptosis and helps us focus on caspase-independent proteases and endonucleases as potential targets of Orf C-induced apoptosis.

Orf C interacts with ANT and Bax

Since a previous study had shown that Orf C targets the cell mitochondria and alters the mitochondrial membrane potential (Nudson et al., 2003), we hypothesized that the pro-apoptotic target of Orf C would reside in the transition pore complex. This hypothesis was based on the knowledge that the mitochondrial membrane potential is controlled in part by the permeability transition pore complex (PTPC) (Kroemer et al., 2007), and thus any membrane potential alterations could be the result of direct interaction with the PTPC. Other viral proteins have been shown to exert apoptotic effects by interacting with these mitochondrial proteins. For example, an HIV-1 accessory protein, Vpr, has been shown to interact with ANT and induce cell death (Boya et al., 2004). The X protein of Hepatitis B virus has also been shown to have pro-apoptotic effects via its interaction with VDAC (Boya et al., 2004).

Given that VDAC and ANT are integral components of the PTPC, we initially conducted experiments to determine if these were the mitochondrial targets of Orf C. While the results did not indicate a role for VDAC in Orf C-induced apoptosis, we did demonstrate that Orf C complexes with ANT (Figure 14). We also examined known pro-apoptotic proteins Bcl-2 and Bax and found that Orf C formed a complex with Bax (Figure 15). Bax is a Bcl-2 family protein that mediates permeabilization of the outer

mitochondrial (OM) membrane and induces apoptosis via disruption of the OM membrane (Kroemer et al., 2007). Under normal cellular conditions Bax is located in the cytosol, but translocates to the OM membrane under specific apoptotic conditions, and can translocate in association with other Bcl-2 family members, Bak or Bid (Kroemer et al., 2007).

While our data indicate that Orf C forms complexes with ANT and Bax, the results were not robust, suggesting that other complexes may be primary inducers of Orf C associated apoptosis. Examples of such proteins could include Bak or Bid that can translocate to the OM membrane with Bax. Further studies are needed to determine if there is a stronger association of Orf C with additional pro-apoptotic proteins.

Orf C localizes to the inner/inter-mitochondrial membrane space

Since we suspected Orf C may not be directly interacting with ANT and/or Bax, we conducted an experiment to narrow the search for other protein(s) of interest that directly target Orf C. To more definitely determine the submitochondrial localization of Orf C we purified mitochondria from Orf C expressing cells and treated them with proteinase K. Since proteinase K digests mitochondrial surface proteins, we could determine if Orf C was interacting with proteins at the outer mitochondrial membrane or the inner/inter-mitochondrial membrane space. We found that Orf C expression remains intact with proteinase K treatment (Figure 16), indicating that Orf C interacts with proteins in the inner membrane or inter-mitochondrial membrane space. This finding is exciting as it significantly narrows the scope of proteins that Orf C may target and

represents significant progress towards determining the mechanism(s) of Orf C-induced apoptosis.

Interaction of Orf C with AIF

Given the previous results we can now focus on proteins located in the inner mitochondrial membrane and/or the inter-mitochondrial membrane space as potential Orf C targets. One specific protein of particular interest is AIF (apoptosis-inducing factor). AIF is located in the inter-mitochondrial membrane space and induces apoptosis via a caspase-independent pathway. Additionally, once it is activated/cleaved from the inter-mitochondrial membrane space it translocates to the cell nucleus where it induces apoptosis by affecting chromatin condensation and DNA fragmentation (Bröker et al., 2005). Since we have observed significant Orf C expression in the cell nuclear fraction we were particularly interested if AIF was activated upon exposure to Orf C.

We examined the mitochondrial, cytosolic, and nuclear cell fractions for AIF expression following exposure to Orf C (Figures 17-19). We were able to detect AIF expression in all cell fractions, with the strongest expression in the mitochondrial and nuclear cell fractions in both experiments. However, to show AIF activation is associated with Orf C, we were looking for AIF expression exclusively in the nuclear extract of the Orf C-expressing cells since AIF translocates to the cell nucleus following activation. Our results did not indicate exclusive AIF activation in the Orf C-expressing cells. However, it did appear that the Orf C-expressing cells showed slightly higher levels of AIF expression in the nuclei in comparison to the negative control cells. This difference

was particularly prominent following the pKH3-Orf C transfections (Figures 18-19). This observation could indicate a possible interaction of Orf C with AIF, however, further studies examining the scope of their interaction is needed to confirm the results.

Future studies examining the role of AIF would include an immunoprecipitation experiment to determine if AIF complexes with Orf C. In addition, other caspase-independent pro-apoptotic proteins should be examined for their role as potential Orf C targets. One such protein is endonuclease G, which upon activation is cleaved from the mitochondria, and then (similar to AIF) translocates to the nucleus where it cleaves chromatin DNA and causes cellular apoptosis (Li et al., 2001; Bröker et al., 2005).

Orf C potential as an oncolytic therapy

Once the mechanism of Orf C-induced apoptosis has been clarified, it will be important to develop an in vivo model to assess the potential use of Orf C as an oncolytic therapy. Our experiments thus far provide much of the groundwork necessary to assess the in vitro oncolytic potential of the Lenti Orf C virus. We have created an ecotropic recombinant lentivirus that expresses Orf C and will be a reasonable method of introducing Orf C into target tumor cells. We have also considered the biosafety aspect of future in vivo studies by creating a virus with an ecotropic envelop that will only infect the target rodent cells (not human cells) and additionally is replication incompetent – avoiding the complications associated with potential systemic infection.

We have also identified an appropriate tumor cell line, the MCA-205 mouse sarcoma cells, as one that is amenable to experimentation with the Lenti Orf C virus. We

have performed extensive experiments demonstrating that these tumor cells undergo apoptosis when infected in vitro with Lenti Orf C.

While the exact mechanism(s) of Orf C-induced apoptosis has not been elucidated, we have made significant progress towards this goal. Once this mechanism has been well defined, Lenti Orf C should be moved into an in vivo experimental mouse model. For the in vivo model we propose using luciferase-expressing MCA-205 cells injected into the mammary fat pad of C57BL/6 mice. Once the tumor cells grow into an easily palpable tumor with an approximate diameter of 0.5 cm, we will inject the tumors with ecotropic Lenti Orf C virus and appropriate controls (ecotropic Lenti empty vector virus or PBS). The tumors will be injected once every three days, for a total of 21 days. Tumors will be imaged at days 7, 14, and 21 with the Xenogen IVIS in vivo imaging system and tumor size will be confirmed via calipers as a secondary measure. On day 21 animals will be euthanized and tissues collected and analyzed for Orf C expression.

The importance of moving forward with an in vivo model is several-fold. First, it is important to determine if the Lenti Orf C virus can effectively reduce tumor size. Second, we also want to assess if a treatment that results in tumor size reduction is associated with an increase in survival time. Finally, one of the most important aspects of conducting an in vivo assessment is to determine if there are any detrimental side effects in the use of Lenti Orf C as an oncolytic therapy. This is especially significant since the apoptosis-induced by Orf C is not specific to tumor cells. Even though it would be injected directly into the tumor cells during treatment experiments, it is possible it could cause ulcerations or other lesions of the cutaneous tissues that would preclude its use as a therapy.

Conclusion

We have successfully completed our first and second specific AIMS. We created a recombinant lentivirus expressing Orf C and used this Orf C-expressing lentivirus to evaluate the in vitro apoptotic potential of Orf C. We have demonstrated the apoptotic properties of our Lenti Orf C virus and specifically identified the MCA-205 mouse tumor cell line as a good model for in vitro, and potentially in vivo, experimentation. We have also shown Orf C expression in the nuclear, mitochondrial, and cytosolic cell fractions, with the most robust levels of expression in the nuclear cell fraction.

We have made significant progress on our third AIM of defining the mechanism(s) of Orf C-induced apoptosis. We have demonstrated that Orf C appears to induce apoptosis via a caspase-independent mechanism. We have also shown evidence that Orf C is associated (perhaps indirectly) with pro-apoptotic proteins ANT and Bax. In addition, we have investigated the effect of Orf C on AIF activation.

Our future study goals are now focused on further characterization of the pro-apoptotic proteins responsible for inducing cell apoptosis via Orf C. We would like to more extensively characterize the relationship between Orf C and AIF, as well as examine an additional pro-apoptotic protein, endonuclease G, that has similar pro-apoptotic characteristics to AIF. By characterizing WDSV Orf C-induced apoptosis, we can more accurately assess the potential of using Lenti Orf C as an oncolytic therapy. Once the mechanism of Orf C-induced apoptosis is well understood, future studies should

move to an in vivo model to assess the potential of Orf C to be used in a clinical treatment capacity.

In summary, we have made significant discoveries regarding the mechanism of Orf C-induced apoptosis. While there are still questions to be answered regarding the unique oncolytic properties of WDSV Orf C, it appears from our initial results that Orf C does have potential to be used as an oncolytic therapy.

References

- Alain T, Hirasawa K, Pon KJ, Nishikawa SG, Urbanski SJ, Auer Y, Luider J, Martin A, Johnston RN, Janowska-Wieczorek A, Lee PW, and AE Kossakowska.** 2002. Reovirus therapy of lymphoid malignancies. *Blood* 100(12):4146-53.
- Altekruse SF, Kosary CL, Krapcho M, Neyman N, Aminou R, Waldron W, Ruhl J, Howlander N, Tatalovich Z, Cho H, Mariotto A, Eisner MP, Lewis DR, Cronin K, Chen HS, Feuer EJ, Stinchcomb DG, Edwards BK (eds).** *SEER Cancer Statistics Review, 1975-2007*, National Cancer Institute. Bethesda, MD, http://seer.cancer.gov/csr/1975_2007/, based on November 2009 SEER data submission, posted to the SEER web site, 2010.
- American Cancer Society** (December 2007). "[Report sees 7.6 million global 2007 cancer deaths](#)". Reuters. <http://www.reuters.com/article/healthNews/idUSN1633064920071217>. Retrieved 2010-09-13.
- Arnold A.** 1995. The cyclin D1-PRAD1 oncogene in human neoplasia. *J Investig. Med.* 43:543-549.
- Begley, S.** (2008-09-16). "[Rethinking the War on Cancer](#)". *Newsweek*. <http://www.newsweek.com/id/157548/page/2>. Retrieved 2008-09-08
- Bowser PR, Wolfe MJ, Forney JL, and GA Wooster.** 1988. Seasonal prevalence of skin tumors from walleye (*Stizostedion vitreum*) from Oneida Lake, New York. *J Wildl Dis* 24:292-8.
- Bowser PR, Martineau D and GA Wooster.** 1990. Effects of water temperature on experimental transmission of dermal sarcoma in fingerling walleyes (*Stizostedion vitreum*). *J Aquat Anim Health* 2:157-61.
- Bowser PR and GA Wooster.** 1991. Regression of dermal sarcoma in adult walleyes (*Stizostedion vitreum*). *J Aquat Anim Health* 3:147-50.
- Bowser PR and JW Casey.** 1993. Retroviruses in fish. *Ann Rev Fish Dis.* 209-24.
- Bowser PR, Wooster GA, Quackenbush SL, Casey RN and JW Casey.** 1996. Comparison of fall and spring tumors as inocula for experimental transmission of walleye dermal sarcoma. *J Aquat Anim Health* 8:78-81.
- Bowser PR, Wooster GA, and K Earnest-Koons.** 1997. Effects of fish age and challenge route in experimental transmission of walleye dermal sarcoma in walleyes by cell-free tumor filtrates. *J Aquat Anim Health* 9:274-278.

- Bowser PR, Wooster GA, Earnest-Koons K, LaPierre LA, Holzschu DL and JW Casey.** 1998. Experimental transmission of discrete epidermal hyperplasia in walleyes. *J Aquat Anim Health* 10:282-6.
- Bowser PR, Wooster GA, Getchell R, Chen C-Y, Sutton C, and Casey J.** 2002. Naturally occurring invasive walleye dermal sarcoma and attempted experimental transmission of the tumor. *J Aquat Anim Health* 14: 288-93.
- Boya P, Pauleau AL, Poncet D, Gonzalez-Polo RA, Zamzami N, and G Kroemer.** 2004. Viral proteins targeting mitochondria: controlling cell death. *Biochimica et Biophysica Acta* 1659:178-89.
- Boya P, Roques B, and G Kroemer.** 2001. Viral and bacterial proteins regulating apoptosis at the mitochondrial level. *EMBO J* 20:4325-4331.
- Brenner C and G Kroemer.** 2000. Mitochondria: death signal integrators. *Science* 289:1150-51.
- Brewster CD, Birkenheuer CH, Vogt MB, Quackenbush SL, and J Rovnak.** 2011. The retroviral cyclin of walleye dermal sarcoma virus binds cyclin-dependent kinases 3 and 8. *Virology* 409: 299-307.
- Bröker LE, Kruyt FAE, and G Giaccone.** 2005. Cell death independent of caspases: a review. *Clinical Cancer Research* 11:3155-3162.
- Crompton M.** 1999. The mitochondrial permeability transition pore and its role in cell death. *Biochem J.* 341:233-49.
- Daniels CC, Rovnak J, and SL Quackenbush.** 2008. Walleye dermal sarcoma virus Orf B functions through receptor for activated C kinase (RACK1) and protein kinase C. *Virology* 375:550-560.
- Earnest-Koons K, Wooster GA, and PR Bowser.** 1996. Invasive walleye dermal sarcoma in laboratory-maintained walleyes (*Stizostedion vitreum*). *Dis Aquat Org* 24:227-32.
- Everett H and G McFadden.** 2001. Viruses and apoptosis: meddling with mitochondria. *Virology* 288:1-7.
- Getchell RG, Wooster GA, and PR Bowser.** 2000a. Temperature-associated regression of walleye dermal sarcoma tumors. *J Aquat Anim Health* 12:189-95.
- Getchell RG, Wooster GA, Rudstam LG, Van De Valk AJ, Brooking TE, and PR Bowser.** 2000b. Prevalence of walleye dermal sarcoma by age class in walleyes

(*Stizostedion vitreum*) from Oneida Lake, New York. *Journal of Aquatic Health* 12:220-223.

Getchell RG, Wooster GA, and PR Bowser. 2001. Resistance to walleye dermal sarcoma tumor redevelopment. *J Aquat Anim Health* 13:228-33.

Getchell RG, Wooster GA, Sutton CA, Casey JW, and PR Bowser. 2002. Dose titration of walleye dermal sarcoma tumor homogenate. *J Aquat Animal Health* 14:247-53.

Green DR and G. Kroemer. 1998. The central executioners of apoptosis: caspases or mitochondria? *Trends in Cell Biology* 8:267-71.

Heibein JA, Goping IS, Barry M, Pinkoski MJ, Shore GC, Green DR, and RC Bleackley. 2000. Granzyme B-mediated cytochrome c release is regulated by the Bcl-2 family members Bid and Bax. *J Exp Med* 192:1391-1401.

Helleday T, Arnaudeau C, and C Lundin. 2005. Recombination repair and a treatment for BRCA2 tumours. *Nature* 434:913-917.

Holzschu DL, Martineau D, Fodor SK, Vogt VM, Bowser PR, and JW Casey. 1995. Nucleotide sequence and protein analysis of a complex piscine retrovirus, walleye dermal sarcoma virus. *J Virol* 69:5320-31.

Holzschu DL, Fodor SK, Quackenbush SL, Earnest-Koons K, Bowser PR, Vogt VM, and JW Casey. 1997a. Molecular characterization of a piscine retrovirus, walleye dermal sarcoma virus. *Leukemia* 11:172-5.

Holzschu, DL, Wooster GA, and PR Bowser. 1997b. Experimental transmission of dermal sarcoma to the saugers *Stizostedion canadense*. *Diseases of Aquatic Organisms* 32:9-14.

Jacotot E, Ravagnan L, Loeffler M, et.al. 2000. The HIV-1 viral protein R induces apoptosis via a direct effect on the mitochondrial permeability transition pore. *J Exp Med* 191:33-46.

Jacotot E, Ferri KF, El Hamel C, et.al. 2001. Control of mitochondrial membrane permeabilization by adenine nucleotide translocator interacting with HIV-1 viral protein R and Bcl-2. *J Exp Med* 193:509-19.

Kesari S, Randazzo BP, Valyi-Nagy T, Huang QS, Brown SM, MacLean AR, Lee VM, Trojanowski JQ, and NW Fraser. 1995. Therapy of experimental human brain tumors using a neuroattenuated herpes simplex virus mutant. *Lab Invest.* 73(5):636-48.

Kolata, G. (April 23, 2009). "[Advances Elusive in the Drive to Cure Cancer](http://www.nytimes.com/2009/04/24/health/policy/24cancer.html)". The New York Times. <http://www.nytimes.com/2009/04/24/health/policy/24cancer.html>. Retrieved 2009-05-05.

Kroemer G, Dallaporta B, and M Resche-Rigon. 1998. The mitochondrial death/life regulator in apoptosis and necrosis. *Annual Rev of Physiology* 60:619-42.

Kroemer G, Galluzzi L, and C Brenner. 2007. Mitochondrial membrane permeabilization in cell death. *Physiol Rev* 87:99-163.

Lakhani SA, Masud A, Kuida K, Porter GA, Booth CJ, Mehal WZ, Inayat I, and RA Flavell. 2006. Caspases 3 and 7: Key mediators of mitochondrial events of apoptosis. *Science* 311(5762):847-51.

Lairmore MD, Stanley JR, Weber SA, and DL Holzschu. 2000. Squamous epithelial proliferation induced by walleye dermal sarcoma retrovirus cyclin in transgenic mice. *PNAS* 97(11):6114-9.

LaPierre LA, Casey JW, and DL Holzschu. 1998. Walleye retroviruses associated with skin tumors and hyperplasias encode cyclin D homologs. *J Virol* 72:8765-71.

LaPierre LA, Holzschu DL, Bowser PR, and JW Casey. 1999. Sequence and transcriptional analyses of the fish retroviruses walleye epidermal hyperplasia virus types 1 and 2: evidence for a gene duplication. *J Virol* 73:9393-403.

Li L, Luo X, and X Wang. 2001. Endonuclease G is an apoptotic DNase when released from mitochondria. *Nature* 412(6842):95-9.

Martineau D, Bowser PR, Wooster GA and LD Armstrong. 1990a. Experimental transmission of a dermal sarcoma in fingerling walleyes (*Stizostedion vitreum vitreum*). *Vet Path* 27:230-4.

Martineau D, Bowser PR, Wooster GA, and JL Forney. 1990b. Histologic and ultrastructural studies of dermal sarcoma of walleye (Pisces: *Stizostedion vitreum*). *Vet Path* 27:340-6.

Martineau D, Renshaw R, Williams JR, Casey JW, and PR Bowser. 1991. A large unintegrated retrovirus DNA species present in a dermal tumor of walleye *Stizostedion vitreum*. *Dis Aquat Org* 10:153-8.

Martineau D, Bowser PR, Renshaw RR, and JW Casey. 1992. Molecular characterization of a unique retrovirus associated with a fish tumor. *Journal of Virology* 66(1):586-99.

Martinou JC and DR Green. 2001. Breaking the mitochondrial barrier. *Nat Rev* 2:63-7.

Mortola E and A Larsen. 2009. Bluetongue virus infection: signaling pathway activated during apoptosis. *Rev Argent Microbiol.* 41(3):134-40.

Nakashima S. 2002. Protein kinase C α (PKC α): Regulation and biological function. *J Biochem* 132:669-675.

Nudson WA, Rovnak J, Buechner M and SL Quackenbush. 2003. Walleye dermal sarcoma virus Orf C is targeted to the mitochondria. *Journal of General Virology* 84:375-81.

Poulet FM, Vogt VM, Bowser PR, and JW Casey. 1995. Insitu hybridization and immunohistochemical study of walleye dermal sarcoma (WDSV) nucleic acids and proteins in spontaneous sarcomas of adult walleye (*Stizostedion vitreum*). *Vet Path* 32:162-72.

Quackenbush SL, Holzschu DL, Bowser PR, and JW Casey. 1997. Transcriptional analysis of Walleye Dermal Sarcoma Virus (WDSV). *Virology* 237:107-12.

Quackenbush SL, Rovnak J, Casey RN, Paul TA, Bowser PR, Sutton C, and JW Casey. 2001. Genetic relationship of tumor-associated piscine retroviruses. *Marine Biotech* 3:S88-S99.

Quackenbush SL, Linton A, Brewster CD, and J Rovnak. 2009. Walleye dermal sarcoma virus rv-cyclin inhibits NF- κ B-dependent transcription. *Virology* 386:55-60.

Reed JC and G Kroemer. 2000. Mechanisms of mitochondrial membrane permeabilization. *Cell Death and Differentiation* 7:1145-55.

Rovnak J, Casey JW, and SL Quackenbush. 2001. Intracellular targeting of walleye dermal sarcoma virus Orf A (rv-cyclin). *Virology* 280:31-40.

Rovnak J, Hronek BW, Ryan SO, Cai S, and SL Quackenbush. 2005. An activation domain within the walleye dermal sarcoma virus retroviral cyclin protein is essential for inhibition of the viral promoter. *Virology* 342:240–251.

Rovnak J and SL Quackenbush. 2006. Walleye dermal sarcoma virus retroviral cyclin directly contacts TAF9. *J of Virology* 80(24):12041-12048.

Rovnak J, Casey RN, Brewster CD, Casey JW, and SL Quackenbush. 2007. Establishment of productively infected walleye dermal sarcoma explants cells. *J Gen Virol.* 88(9): 2583-2589.

Rovnak J and SL Quackenbush. 2010. Walleye dermal sarcoma virus: molecular biology and oncogenesis. *Viruses* 2:1984-1999.

- Salvesen GS and SJ Riedl.** 2008. Caspase mechanisms. *Adv. Exp. Med. Biol.* 615:13-23.
- Sherr CJ.** 1995. D-type cyclins. *Trends Biochem. Sci.* 20:187-190.
- Walker R.** 1969. Virus associated with epidermal hyperplasia in fish. *Natl. Cancer Inst. Monogr.* 31:195-207.
- Yamamoto T, MacDonald RD, Gillespie DC, and RK Kelly.** 1976. Viruses associated with lymphocystis and dermal sarcoma of walleye (*Stizostedion vitreum vitreum*). *J Fish Res Board Can* 33:2408-2419.
- Yamamoto T, Kelly RK, and O Nielsen.** 1985a. Epidermal hyperplasia of walleye, *Stizostedion vitreum vitreum* (Mitchell), associated with retrovirus-like type-C particles: prevalence, histologic and electron microscopic observations. *Journal of Fish Diseases* 8(5):425-36.
- Yamamoto T, Kelly RK, and O Nielsen.** 1985b. Morphological differentiation of virus-associated skin tumors of walleye (*Stizostedion vitreum vitreum*). *Fish Path.* 20:361-72.
- Yuan S, Yu X, Topf M, Ludtke SJ, Wang X, and CW Akey.** 2010. Structure of an apoptosome-procaspase 9 CARD complex. *Structure* 18(5):571-83.
- Zamzami N and G Kroemer.** 2001. The mitochondrion in apoptosis: How Pandora's box opens. *Nat Rev* 2:67-71.
- Zhai Y, Yang JC, Kawakami Y, Spiess P, Wadsworth SC, Cardoza LM, Couture LA, Smith AE and SA Rosenberg.** 1996. Antigen-specific tumor vaccines: Development and characterization of recombinant adenoviruses encoding MART1 or gp100 for cancer therapy. *J Immunol.* 156(2):700-10.
- Zhang A and D Martineau.** Walleye dermal sarcoma virus: Orf A N-terminal end inhibits the activity of a reporter gene directed by eukaryotic promoters and has a negative effect on the growth of fish and mammalian cells. *J Virol.* 73(10):8884-9.